Tellus SERIES B CHEMICAL AND PHYSICAL METEOROLOGY
PUBLISHED BY THE INTERNATIONAL METEOROLOGICAL INSTITUTE IN STOCKHOLM

Long-term trends of mono-carboxylic acids in Antarctica: comparison of changes in sources and transport processes at the two EPICA deep drilling sites

By M. DE ANGELIS[1]*, R. TRAVERSI[2] and R. UDISTI[2], [1]*UJF – Grenoble 1/CNRS, LGGE UMR 5183, Grenoble, France;* [2]*Chemistry Department, University of Florence, Florence, Italy*

(Manuscript received 26 May 2011; in final form 25 January 2011)

ABSTRACT

We present here the first profiles of acetate and formate concentrations in Antarctic ice for time periods that include the great climatic changes of the past. Data are from two Antarctic deep ice cores recovered on the central East Antarctic Plateau (EDC) and in the Dronning Maud Land (EDML) facing the Atlantic Ocean (European EPICA Project). Except the sporadic arrival of diluted continental plumes during glacial extrema, the main source of acetate deposited over the EDC does not seem to have changed significantly over the past 300 kyr and is related to marine biogenic activity. A more detailed study of the past 55 kyr leads to the conclusion that acetate reaching the EDML during a large part of the last glacial maximum was emitted by the Patagonian continental biomass and was uptaken along with nitric acid at the surface of mineral dust. Changes in formate concentrations are characterised by less scattered and lower values at both sites during glacial periods. We propose that the present marine source of formic acid (Legrand et al., 2004) drastically decreased but did not completely vanish under cold climate conditions, whereas the share of methane oxidation in formic acid production became prominent.

Keywords: ice cores, polar atmosphere, formic acid, acetic acid, climatic cycles

1. Introduction

1.1. Background – atmosphere

Carboxylic acids are one of the dominant classes of organic compounds found in the atmosphere and significantly contribute to the non-methane hydrocarbons (NMHC) atmospheric content. They have been studied in a wide variety of environments under tropical and mid-latitudes (see Chebbi and Carlier, 1996; Khare et al., 1999, for detailed reviews). Weak organic acids are distributed worldwide in the troposphere and, in addition to sulphuric and nitric acids, they play a prominent role in the aqueous and gaseous phases of the atmospheric acidity. Their role in tropospheric chemistry through cloud chemistry and precipitation acidity is particularly important, especially in remote regions. Formic and acetic acids, mainly present in the gaseous phase (Talbot et al., 1988), are by far the most abundant carboxylic acids in the global troposphere (Keene and Galloway, 1984, 1988). They largely dominate the gaseous phase of urban-polluted, rural, remote continental and marine atmospheres. Despite great spatial variability, they remain predominant in aqueous phases (rain, fog, snow and ice samples), where significant amounts of di-carboxylic acids are also observed.

Sources of light carboxylic acids (formic and acetic) are now fairly well recognised and include primary anthropogenic biofuel and fossil fuel emissions (Talbot et al., 1988; Grosjean, 1992; Chebbi and Carlier, 1996; Khare et al., 1999), biomass burning (Talbot et al., 1990; Lefer et al., 1994), direct emissions from soil and vegetation (Kesselmeier and Staudt, 1999) and photochemical production (Madronich et al., 1990). The main reactions producing light carboxylic acids in the atmospheric gaseous phase are: (1) the ozone oxidation of olefins emitted from soil and vegetation (isoprene, monoterpene, Jacob and Wofsy, 1988) as well as in the marine atmosphere by biogenic precursors (light alkenes, Keene and Galloway, 1988; Bonsang et al., 1991; Koppman et al., 1992; possibly isoprene, Bonsang et al., 1992), (2) the reactions of peroxyl and proxy acetyl radicals producing acetic acid in

*Corresponding author.
email: mdeangelis@lgge.obs.ujf-grenoble.fr

Tellus B 2012. © 2012 M. De Angelis et al. This is an Open Access article distributed under the terms of the Creative Commons Attribution-Noncommercial 3.0 Unported License (http://creativecommons.org/licenses/by-nc/3.0/), permitting all non-commercial use, distribution, and reproduction in any medium, provided the original work is properly cited.
Citation: Tellus B 2012, **64**, 17331, DOI: 10.3402/tellusb.v64i0.17331

moderately polluted atmospheres (low NO_x concentrations, Madronich and Calvert, 1990) and (3) the oxidation of methane by OH-producing HCOOH in remote areas (Jacob, 1986). The atmospheric chemistry of formaldehyde in aqueous phase via OH radicals is an important source of formic acid, but cloud water can act both as a source or sink of formic acid in the gaseous phase depending on its pH. However, key questions concerning the atmospheric budgets of formic and acetic acids like the nature and relative importance of individual sources as well as the partitioning between natural and anthropogenic sources remain open. Typically, the long-range transport and lifetime of precursors emitted by intense tropical biomass burning strongly influence the cycle of organic species over wide oceanic areas (Herman et al., 1999; Singh et al., 2000). The existence of a long-lived secondary source of monocarboxylic acid, very likely associated with aerosol ageing, accounting for ca. 50% of global sources, was proposed by Paulot et al. (2011), following their detailed budget of formic and acetic acids. Moreover, little is known on the sinks of light carboxylic acids: wet deposition is considered to be the largest sink of these two species (Chebbi and Carlier, 1996) but in-cloud processes driving their incorporation into solid or liquid precipitation have not been fully investigated (Voisin et al., 2000; Paulot et al., 2011) and their residence times, controlled by precipitation rate, are not well known and may be of a few days or a few weeks (Keene and Galloway, 1988; Jacob and Wofsy, 1988; Talbot et al., 1988; Paulot et al., 2011). The heterogenous uptake by dust does not seem to be a major sink at a global scale but may play a prominent role in the vicinity of large arid areas (Al-Hosney et al., 2005; Hatch et al., 2007).

Since the mid-1990s, investigations have been carried out on North and South polar ice caps with the aim of better characterising the present natural sources of carboxylic acids in very remote areas. Typical mixing ratios of formic and acetic acids for Greenland and Antarctic atmospheres are shown in Table 1. Data were gained by: (1) year-round sampling of aerosol and gaseous phases at Dumont D'Urville, a site located on the East Antarctic coast (Legrand et al., 2004); (2) gas sampling in the summer of 2000 at South Pole (Dibb and Arsenault, 2002; Eisele et al., 2008) and (3) gas sampling in the summer of 1993 (Dibb et al., 1994), 1995 (de Angelis, unpublished data) and 2000 (Dibb and Arsenault, 2002) at Dome Summit, Greenland.

Greenland is surrounded by wide continental areas with limited oceanic influence. The main sources of carboxylic acids for Central Greenland lie in North America and Asia, from where air trajectories reach the ice cap after a very short track over the North Atlantic, especially over the Arctic Ocean (Kahl et al., 1997). This offers the possibility to better approach the part of the carboxylic cycle related to natural continental sources (biomass burning from the boreal forest, and biomass and soil emission from lower latitudes (Currie et al., 2005). On the contrary, Antarctica is surrounded by a very vast expanse of ocean, so the continental influence remains very restricted under the present climate conditions. However, while coastal sites may be considered to be very remote marine sites, two types of air masses are expected to reach more central sites: aged marine air masses transported at high altitude, in the

Table 1. Mean concentrations of acetic end formic acids in the gaseous phase of recent polar atmosphere

Site	Acetic A. pptv	Formi c A. pptv	Season	Period	Year	
Greenland						
Summit						
(1)	390	670	Summer	06/06–07/20	1995	De Angelis, unpublished data
(2)	230	420		06/06–06/16		
(3)	560	720		06/17–06/27		
(4)	630	1300		06/28–07/10		
Summit	715	1100	Summer	06/20–07/19	1993	Dibb et al. (1994)
Summit	445	460	Summer	06/04–07/07	2000	Dibb and Arsenault (2002)
Antarctica						
D. D'Urville	60	65	Winter	April–October	1997–2002	Legrand et al. (2004)
	380	170	Summer	November–March		
South Pole	230	70	Summer	12/01–12/15	2000	Eisele et al. (2008)
	275	125		12/16–12/31		
	310	159	Summer	12/14–12/28	2000	Dibb and Arsenault (2002)

Concentrations are expressed in pptv. De Angelis, unpublished data: (1) mean concentrations calculated over the whole sampling period; (2) background mean concentrations – beginning of the field season; (3) and (4) mean concentrations of two successive broad peaks observed during the second part of the field season.

buffer layer or the free troposphere where additional physicochemical reactions may occur (Preunkert et al., 2008), and diluted continental plumes. This is proven by the analysis of aerosol samples taken at Amundsen Scott – South Pole Station from 1979 to 1983 (Tuncel et al., 1989), which has shown that crustal particles are transported from lower Southern latitudes to the South Pole atmosphere within the mid-troposphere, essentially during summer. Thus, studies performed at central East Antarctic sites may provide the opportunity to also investigate the influence of very long-range transport from continental sources.

Acetic and formic acids are mainly present in the gaseous phase in polar regions (Dibb et al., 1994; Legrand et al., 2004). In the Antarctic coastal atmosphere, the concentrations of formic and acetic acids are characterised by a great inter-annual variability. Legrand et al. (2004) concluded that the main source of acetic acid is the photochemical degradation of dissolved organic carbon (alkane, alkene) emitted from the Antarctic Ocean. This is also valid for formic acid in the winter, whereas in the summer an additional and still unknown source must be considered. Very scarce data are available for the Central Plateau: as shown in Table 1, December concentrations at South Pole are in the same range as the mean summer value at Dumont D'Urville. This may suggest that the long-range transport of acetic and formic acids tends to homogenise corresponding mixing ratios over wide areas. Mean values of gas concentrations of acetic and formic acids measured a few metres above the snow surface in Central Greenland are in the same range (de Angelis, unpublished data; Dibb and Arsenault, 2002) or even higher (Dibb et al., 1994) than those previously reported for high latitude continental sites. Data published by Dibb et al. (1994) correspond to samples collected during four separate sampling runs covering a few consecutive days each, and a strong decreasing trend (factor 4) of both acids may be observed from the beginning to the end of the experiment. In the other two studies, samples were collected continuously (24 h/d, de Angelis, unpublished data) or semi-continuously (interrupted at night, Dibb and Arsenault, 2002) over time periods indicated in Table 1. Background concentrations (i.e. regardless of large perturbations, de Angelis, unpublished data) of acetic acid over Central Greenland are in the same range as summer concentrations at coastal and central Antarctic sites, whereas formic to acetic acid ratios are several times higher, whatever the dataset taken into account, very likely in relation with the quasi-permanent influence of biomass combustion in the remote Northern Hemisphere in summer and the formation of formic acid in ageing fire plumes (Legrand and de Angelis, 1995; Legrand et al., 2003; Paulot et al., 2011).

1.2. Input of ice cores to the current understanding of carboxylic cycles

Since the early 1960s, ice core analyses have provided a wealth of reliable concentration depth profiles and allowed preliminary paleo-atmospheric reconstructions. Multiparameter approaches, aiming to investigate the role of the air – snow transfer function and of post-deposition processes occurring at the snow surface in the building of chemical ice archives, were initiated more recently: the influence of precipitation acidity on the incorporation of formic and acetic acids present in the gaseous phase is visible in Greenland (Legrand and de Angelis, 1995); post-depositional relocation of acetate and formate peaks have been observed in freshly fallen snow at central Greenland sites (De Angelis and Legrand, 1995; Dibb et al., 1994); significant depletion of other reactive gases (HNO_3 and HCl) seems to occur within the uppermost firn layer at central Antarctic sites (e.g. De Angelis and Legrand, 1995) in relation with temperature and/or annual snow accumulation rate: the lower the accumulation rate, the higher the post-deposition loss (Weller et al., 2004; Traversi et al., 2009). On the other hand, apart from the direct incorporation of reactive gases into precipitation, alternative pathways are chemical reactions leading to the formation of non-reversible aerosol or dry deposition at the surface of particles transported over ice caps. It is obvious that the interpretation of ice core profiles will be progressively improved by a better knowledge of atmospheric interactions and air – snow exchanges. However, providing reliable concentration profiles is a key step in the understanding of past environmental changes, and we feel that the lack of information concerning the air – snow transfer function must not rule out qualitative discussions on innovating data.

The first detailed investigation of carboxylates (acetate, formate, glycolate and oxalate) in Central Greenland ice cores (Dome Summit, 72°34′S, 37°38′W, 3240 m above sea level) demonstrates that high latitude vegetation emission and biomass burning events represent the major contributors to the carboxylic acid budget in snow cover at high Northern latitudes (Legrand and de Angelis, 1995, 1996). Background levels strongly decreased during the glacial age in relation with the formation of the Laurentide ice sheet and the corresponding decrease in the vegetation emission from North America: at that time, it is likely that the part taken by the marine source in carboxylic emission became significant. A very high-resolution study performed over the last millennium at the same site (Savarino and Legrand, 1998) enabled the authors to assess fire frequency and intensity, by relating the relative abundance of ammonium and nitrate compared with formate in ice layers containing

fire debris to the flaming or smouldering character of the event.

Data were more recently obtained along ice cores from lower latitudes, providing additional information on remote continental sites of the Northern and Southern Hemispheres. Based on high-resolution records of formate and acetate from a high altitude Alpine glacier (Col du Dome, 4250 m above sea level, French Alps, Legrand et al., 2003), it was concluded that in addition to convective transport from the boundary layer, secondary production of formic and acetic acids in the troposphere may contribute to the carboxylic acid budget in the mid-troposphere over Europe. However, the contribution of anthropogenic emissions remains weak even over populated areas (Paulot et al., 2011; Legrand et al., 2003). The detailed study of two cores extracted from a cold, high altitude site of the Northern Patagonian ice cap (Monte San Valentin, 46°35′S, 73°19′W, 3747 m above sea level, Vimeux et al., 2008; Moreno Rivadeneira 2011) shows the regular occurrence of aerosol and gaseous compounds from soil emissions and burning events. Deposits related to burning events are characterised by large increases in ammonium and nitrate in the same range as in Greenland ice impacted by fire plumes, whereas non-sea-salt sulphate concentrations and snow acidity are markedly higher, very likely in relation with fuel characteristics. Indeed, varying and sometimes large amounts of SO_2 and sulphate have been measured during experimental burns of wild or agricultural biomass (Keene et al., 2006; Tissari et al., 2008). The increase of di-carboxylates is moderate and the concentrations of acetate and formate remain low as previously observed in Greenland acidic ice layers (Legrand et al., 1995).

Only one formate record is available for Antarctica (Legrand and de Angelis, 1995). Discontinuous measurements were made along a 307-m long ice core recovered in Adelie Land, at a site located 5 km from the coast and facing Dumont D'Urville (D10, 66°40′S 139°49′E, 270 m above sea level). Due to contamination problems, other species of interest (ammonium, acetate) were not measured. Formate concentrations measured along the part of the core corresponding to early Holocene precipitation are one order of magnitude lower than in Greenland. Concentration levels in ice from the glacial age are lower by a factor close to five than in Holocene samples. Authors conclude that formate concentrations are mostly related to in-cloud oxidation of formaldehyde derived from methane oxidation. Although the origin of the ice along the D10 core remains uncertain due to ice folding, sodium concentrations at the beginning of the Holocene are similar to concentrations measured in surface samples taken 300–500 km inland (ca. 2000 m above sea level) along the flow line (Briat et al., 1974). Thus, it appears relevant to consider that the conclusion of Legrand and de Angelis (1995) is valid for the edge of the East Antarctic Plateau (EDC).

1.3. What can be expected from EPICA deep ice cores?

Two ice cores were recovered during the deep drilling European Project for Ice Coring in Antarctica (EPICA) at sites experiencing relatively large differences in meteorological conditions and sources apportionment: the first core was drilled at Dome C on the EDC (75°06′S, 123°21′E, 3233 m above sea level) and covers the past 800 kyr. The second one was drilled in the Dronning Maud Land (EDML) at Kohnen Station (75°S, 0°E, altitude 2892 m above sea level) facing the Atlantic Ocean. The Holocene part of the cores will offer the possibility to investigate mainly the contribution of the marine source. Regarding the continental contribution to the snow archive, a rough estimate can be made by considering that soil particles account for only 5% of the mass of sea-salt aerosol at South Pole in winter (Tuncel et al., 1989) and 30% in summer (Kumai, 1976). Note that this moderate influence of the continental component is in agreement with aerosol studies performed at South Pole in 1998 and 2000 and shows that ^{210}Pb activity in South Pole aerosol is lower by roughly two orders of magnitude than what is observed in tropical areas (Preiss et al., 1996; Arimoto et al., 2004). Based on sodium concentration in South polar snow (e.g. Wolff et al., 2006) and the relative abundance of calcium in continental soils and marine primary salt, the estimate of non-sea-salt calcium (continental indicator in studies performed by ionic chromatography, see Section 3) for present climate conditions remains in the ng g^{-1} range, which is very low. On the other hand, the prominent part that the dust input from Patagonian sources represents compared with the marine contribution over Central Antarctica during the glacial age (Gaudichet et al., 1992; Basile et al., 1997; Delmonte et al., 2003) raises an interesting question: did any significant contribution from the Patagonian biomass reach Antarctica along with air masses transporting soil dust at that time? Data from the glacial part of the cores may help to answer this question.

The study presented here is focused on acetate and formate discontinuous depth profiles established along EDC and EDML ice cores. It provides the first comprehensive investigation of mono-carboxylic acids along Antarctic ice cores. The relationships likely link acetate and formate with species considered to be valuable although intricate markers of aerosol and gas sources for Antarctica are assessed by comparing concentration depth profiles and by inter-correlation calculations. These source

markers are: sodium (marine primary aerosol), ammonium (plankton activity, soil biogenic emissions, biomass burning), non-sea-salt calcium (arid and semi-arid soil), non-sea-salt sulphate (marine biogenic dimethylsulphide [DMS], volcanism), nitrate (soil emission, biomass burning) and methane (formaldehyde and thus a formate precursor). We are aware that the lack of information on the air – snow transfer function temporarily prevents identification of a quantitative relationship between snow and atmospheric composition. Nevertheless, valuable information on the past continental biomass has been provided by the Greenland Summit ice cores despite a very similar caveat (Legrand and de Angelis, 1995, 1996; Savarino and Legrand, 1998). Moreover, concentration profiles presented here come from two sites influenced in very different ways by remobilisation processes (Traversi et al., 2009; Weller et al., 2004) so that comparing the two datasets may improve their significance. Thus, we propose a preliminary interpretation of specific events and profile trends identified along EDC and EDML in terms of origin and removal processes for the part of acetic and formic acid stored in ice archives.

2. Analysis

The way ice core samples are reprocessed to investigate trace species is critical in obtaining a reliable set of data. Major contamination of the outer part of deep ice cores occurs during drilling, particularly when drilling fluid is used. Additional contamination is introduced through core handling and cutting in the field as well as during core storage. This is particularly true for organic species, which are very sensitive to contamination. Organic contaminants are ubiquitous: in drilling fluid, in plastic material used for core wrapping and in the atmosphere. They are known to progressively diffuse from the outer part to the inner part of ice sections (e.g. Savarino and Legrand, 1998). Moreover, even under clean room conditions, it is very difficult to prevent gaseous contamination during the analytical step: exchanges between samples and surrounding air or material (vial, sampling syringe) may become significant compared with the concentration range of sensitive species, such as acetate, formate or ammonium. Thus, the profiles presented here required overcoming some major difficulties: cleaning the samples, improving analytical conditions and carefully checking the data.

Discrete samples were successively cut in the most inner part of every ice piece with a band saw, scraped with a razor blade and rinsed in three successive baths of ultra pure water. Strong methane sulphonate (MSA) depletion was observed in Antarctic ice samples that were rinsed after their temperature was allowed to rise close to 0 °C to avoid thermal cracks (M. Legrand, personal communication). To avoid such losses, our samples were kept cold (i.e. below −10 °C) before rinsing and the rinsing procedure was very rapid. The comparison with samples that underwent mechanical reprocessing alone demonstrated the good preservation of MSA in our samples. This kind of comparison was not possible for species that are very sensitive to contamination like carboxylates, but given the high mobility of MSA in ice lattice, a good preservation of other weak acids can be expected. Samples were kept in frozen state and stored in air-tight glass bottles (Schott®) until analysed.

Measurements were performed by ion chromatography. Acetate and formate concentrations were systematically higher in water aliquots analysed with an auto sampler than in similar samples that were manually injected. The contamination increased with the time the samples were stored in the auto sampler and was often in the same range as sample concentrations for formate, whereas it was generally lower than the detection limit in manually injected samples. Thus, we decided to use only manual injection. Calibration curves were established every day using artificial standard solutions of known composition prepared just before injection. The analytical uncertainty was deduced from the scattering of the signal of individual standards around every calibration curve. It remained lower than a few percent for mineral ions. Formate and acetate concentrations in standard solutions ranged between 0.2 and 5 ng g^{-1}. Calibration scattering, and thus analytical uncertainty, was increased by the quite moderate but varying gaseous contamination introduced by the dilution step. Scattering values around formate and acetate calibration curves typically ranged between approximately 0.05 and 0.1 ng g^{-1}, leading to analytical uncertainty ranging from a few percent to up to around 50% depending on daily analytical conditions and sample concentrations.

Two kinds of ice sections were successively reprocessed. At first, we were allowed to use only ice lamellae selected among the set of ice sections attributed to the LGGE as part of the high-resolution ion chromatography (IC) analysis of the EDC core (Littot et al., 2002). These ice sections, called chemistry strips, were 55 cm long and taken from the very outer part of the core. Due to their location and thinness, the rapid decontamination procedure developed for high-resolution analyses proved inadequate even for major ions. Thus, in the second step, that is, below 580 m along the EDC core, high-resolution ion chromatography was performed on samples recovered by on-line melting of a more inner lamella (Wolff et al., 2006) and samples devoted to organic studies were separate ice pieces cut on a central lamella of the core and wrapped in aluminium foil until decontamination and analysis could take place. This sampling procedure was used along the whole EDML ice.

2.1. EDC 0 – 580 m

A first set of chemistry strips randomly chosen among those attributed to the LGGE was reprocessed and analysed in 2001 and 2002. Every ice section was mechanically decontaminated and then subsampled in successive ice pieces, 6–8 cm long, which were individually rinsed in three successive baths of ultra pure water. A preliminary experiment was conducted as part of the high-resolution chemistry programme, aiming to check the rapid decontamination procedure. It provided useful information on contaminant species. In this experiment, only 2–3 mm of ice was directly removed with a plane from the surface of every strip before subsampling. Ammonium, potassium, acetate, formate, oxalate and calcium concentrations one order of magnitude higher, or even more, than maximum concentrations found in strips decontaminated for organics were found in some of these samples. These very high concentrations were associated with huge amounts of another ion identified as lactate. The frequent occurrence of this quite anomalous concentration pattern clearly demonstrated that the rapid decontamination procedure was inadequate and led us to focus on lactate. Although lactate concentrations as high as several tens of $ng\,g^{-1}$ were observed in samples from EDC strips not adequately decontaminated (1) they remained below the detection limit in Greenland ice lamellae taken in a more central part of the core and immediately reprocessed in the field, (2) only moderate lactate concentrations were occasionally observed in ice cores from tropical cold glaciers strongly influenced by continental sources (de Angelis, unpublished data) and (3) lactate concentrations in all our analytical blanks were below the detection limit. Thus, we considered the presence of lactate in our samples, even at very low concentration levels, to be related to relic contamination liable to have affected other ions, including carboxylates. The decontamination efficiency was then checked by combining two criteria: (1) the variability of acetate and formate concentrations observed along each lamella and (2) the absence of lactate. Along a given lamella, acetate and/or formate concentrations greater than (c_{mean} + SD) (where c_{mean} and SD are the concentration mean value and corresponding standard deviation (SD) calculated for the whole lamella) were considered as outliers and carefully scrutinised. Samples with formate outliers account for $<3\%$ of the whole set of samples. In all these samples, acetate outliers were also observed. Ca. 70% of samples with formate outliers are located at bag extremities where contamination risks are obviously greater due to increased surface exposure to contamination compared with sample volume. Samples with formate outliers not located at bag extremities account for $<1\%$ of the whole set of samples. Samples with acetate outliers account for 28% of the whole set of samples. Forty percent of acetate outliers were observed in samples located at bag extremities. In all corresponding chromatograms, acetate peaks were partly hidden by lactate peaks. Significant amounts of lactate not located at bag extremities were also observed in a large part of samples with acetate outliers, and lactate remained below the detection limit in samples not identified as outliers. We are aware that discarding all samples containing lactate may seem excessive, but the link between acetate outliers and lactate traces supports the choice of lactate as a contamination marker. The remaining samples with acetate outliers (roughly 7% of the whole set of samples) did not show any specific trend along the core. They may correspond either to a few particular events or to contamination traces. We decided to discard these samples also, mainly because, even if tracking true events, they were too scarce to allow any statistical approach and we preferred to focus our study on background trends. In Fig. 1, we present the distribution of acetate concentrations before and after samples considered to be contaminated have been rejected. This figure shows that the main characteristics of background distributions are not significantly modified by the sorting procedure. Although difficult and time consuming, this first step notably improved the quality of the sampling procedure for high-resolution ion chromatography as well as for organic studies. Acetate concentrations found in the remaining part of chemistry strips reprocessed and analysed in 2004 or 2005 were higher and much more scattered than previous data because of acetate diffusion through ice pieces stored for three additional years. They were not taken into account in this study.

2.2. EDC 580–2400 m and EDML

Ice lamellae available during the second part of our study were central lamellae, several centimetres thick. These ice

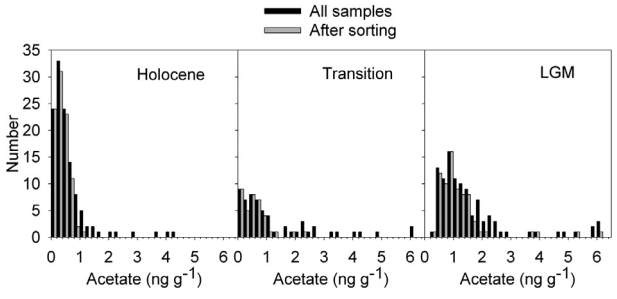

Fig. 1. Acetate concentration distributions obtained along the 580 upper metres of EDC and corresponding to the Holocene (left), last glacial – interglacial transition (middle) and LGM (right) time periods. Black bars refer to the whole set of samples and grey bars refer to samples estimated to be reliable, following the sorting procedure described in Section 2.

sections were never in direct contact with drilling fluid and their surface was much cleaner than the surface of chemistry strips. Moreover, the size of ice sections enabled us to remove ca. 1 cm on every side of the lamellae. This considerably improved the efficiency of the decontamination step. Only one sample was taken from each lamella. In conformance with our sorting criteria, samples containing lactate traces were discarded.

2.3. Summary

EDC data taken into account in the discussion correspond to chemistry strips after outliers have been discarded (0–580 m, this part of the core covers the past 30 kyr) and discrete samples taken every 10 m along more central ice sections after samples containing lactate have been discarded (this part of the core, 580–2400 m, covers from 300 to 30 kyr before present, noted BP). EDML data correspond to 10-cm long sections of ice lamellae taken every 4 m between 450 and 1560 m. All samples were measured within a few weeks under very similar analytical conditions. The time period covered includes a large part of the Holocene and the glacial age back to ca. 55 kyr BP.

3. Results and discussion

3.1. Recent snow as a reference

Concentration profiles obtained along a 160-cm deep pit dug and sampled during the 1997–1998 field season at Dome C made it possible to check the efficiency of the decontamination process and provided very preliminary information on the deposition pathway of carboxylic acids under present climate conditions. Depth-concentration profiles of acetate, formate and oxalate are shown in the left part of Fig. 2. In the right part of the figure, we present concentration profiles of the non-sea-salt component of calcium [$nssCa = Ca - (Ca/Na)_{sea\ water} * Na$], ammonium and the non-sea-salt component of sulphate [$nssSO_4 = SO_4 - (SO_4/Na)_{sea\ water} * Na$]. The seawater composition is from Keene et al. (1986). Long dashed lines correspond to concentration ranges measured along the Holocene part of the core.

The large peak of $nssSO_4$ observed at a depth of 42–52 cm was attributed to the arrival of stratospheric aerosols emitted by the Pinatubo eruption in 1992–1993 (June 1991). This corresponds to a 10 cm yr^{-1} snow accumulation rate and leads to date the bottom of the pit in 1980.

Background concentrations of all species except nss sulphate increase from the bottom of the pit to the surface. In addition to this common general trend, simultaneous occurrences of sharp concentration peaks noted as A, B, C, D and E in Fig. 2 can be observed: (A) in the surface layer (acetate, formate, ammonium, oxalate, nss calcium), (B) at 37–42 cm (acetate, formate, ammonium), (C) at 58–62 cm (acetate, formate, ammonium, oxalate, nss calcium, nss sulphate), (D) at 76–81 cm (formate, ammonium, oxalate, nss sulphate) and (E) at 81–85 cm (acetate, nss calcium). Formate to acetate molar ratios vary between 0.2 and 0.9

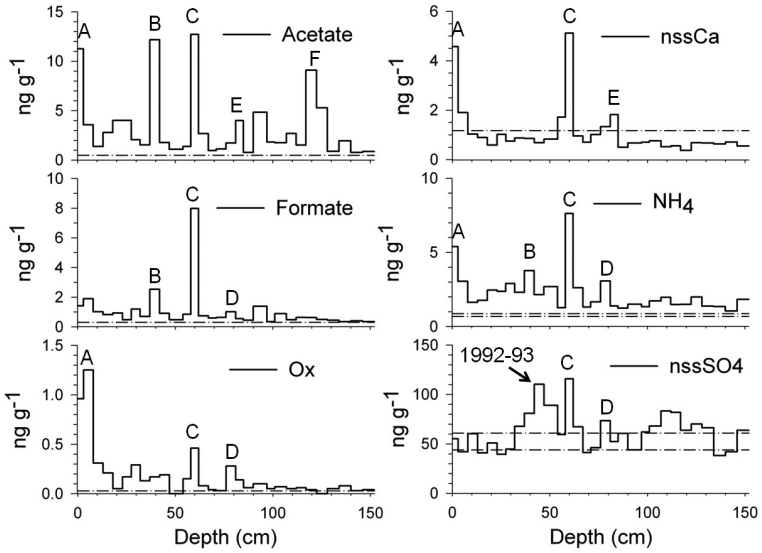

Fig. 2. Concentration depth profiles of acetate, formate, oxalate (left, from top to bottom, respectively), nss calcium, ammonium and nss sulphate (right, from top to bottom, respectively) along a 160-cm pit dug in summer 1997–1998 at DC site. The white dash-dotted lines on each graph delineate the range of Holocene values (Holocene mean value ± SD, when corresponding to a negative value the lower line is not shown). The time scale is given by the nss sulphate peak centred at 42–52 cm deep and attributed to Pinatubo stratospheric deposits in 1992–1993. See text for concentration peaks marked A, B, C, D, E and F.

with a maximum value in peak C. Based on ionic equilibrium, it may be suggested that acetate, formate and oxalate are present as ammonium salts in peaks A, B and C accounting for 80–100% of ammonium concentrations. This is not the case in peak D, where ca. 70% of ammonium content is very likely neutralised by biogenic sulphate. The snow layer corresponding to peak B is located within the thicker layer largely impacted by Pinatubo stratospheric deposits making it difficult to evidence any additional contribution of marine biogenic sulphate. However, it seems reasonable to propose that concentration peaks B and D correspond to sporadic events of biogenic marine origin. The 58–62 cm snow layer (peak C) contains large amounts of nss sulphate accompanied by nss calcium, mono- and di-carboxylates, ammonium and MSA (not shown here). Ammonium and formate concentrations are particularly high. This snow layer is located just below the level corresponding to the 1992–1993 Pinatubo event, and thus should contain aerosol emitted by the Cerro Hudson eruption in August 1991, because, in late 1991, a significant pole-ward transport of the Cerro Hudson sulphate aerosol in the lower stratosphere beneath the polar vortex and possibly in the middle/upper troposphere was observed at coastal Antarctic sites (Legrand and Wagenbach, 1999). The volcanic plume may have reached more central areas at the time the vortex weakened providing them with unusually high amounts of mineral particles and ashes, among them aged combustion products from post-eruption smouldering events. The presence of MSA suggests that reactions involving marine reactive gases present in the Antarctic troposphere in late spring/early summer have occurred at the surface of volcanic debris. The association of acetate and nss calcium in peak E may be explained by the mixing of marine and continental air masses promoting heterogeneous uptake of marine reactive gases on continental alkaline aerosol during transport (Dentener et al., 1996; Al-Hosney et al., 2005; Hatch et al., 2007), by a common continental origin of these species or by a combination of these two causes. The deepest acetate peak at 117–128 cm (F) is located at the same depth as a slightly wider sodium peak (112–128 cm, not shown here).

Similarities in background trends and peak occurrences observed for acetate/formate, expected to have been incorporated as reactive gases, and species known to be associated with non-volatile aerosol (ammonium, oxalate, nss calcium, sodium), suggest that: (1) a significant part of acetate/formate deposited in snow under present climate conditions may result from interactions between acetic/formic acids and alkaline aerosol of continental or marine origin during transport or within the snow; (2) concentration increases of formate and acetate background observed in more recent snow layers could be related to the changes that have occurred in aerosol load over Dome C since the 1980s, possibly in relation with increasing scientific and logistic activity rather than to post-depositional losses.

Concentrations at the bottom of the pit are quite similar to Holocene values except for acetate and ammonium, which remain slightly higher. The seasonal-like variations of carboxylate observed in Central Greenland remained of same amplitude and frequency over a large part of the last millennium (Savarino and Legrand, 1998) leading to the thought that incorporation mechanisms do not significantly change at a given site under stable climate conditions. We can safely assume that present climate conditions at Dome C are very close to the mean Holocene ones. Thus, the close agreement between concentrations found at Dome C in the deepest part of the pit and Holocene mean values is a strong argument in favour of decontamination efficiency.

3.2. *Acetate*

EDC nss calcium, sodium, nss sulphate, ammonium and acetate depth profiles are shown in the left part of Fig. 3, where the climate reference is given by the deuterium profile (EPICA Community Members, 2006). The time scale is indicated on every upper axis. EDML corresponding profiles are shown in the right part of Fig. 3, from top to bottom, respectively. The time scale from Ruth et al. (2007) is indicated on the upper axis of every graph, and climate references for the past 50 kyr are indicated on the sodium graph. The grey dots (EDC) and thin black lines (EDC and EDML) refer to concentrations expressed in $\mathrm{ng\,g^{-1}}$ on left axes, and the thick black lines to the corresponding five sample running means.

Based on an extensive study of deposition fluxes, Legrand (1995) and de Angelis et al. (1997) concluded that, under stable climate conditions and over wide areas of polar ice caps influenced by well-homogenised air masses, dry deposition velocity and scavenging ratios for precipitation of nss sulphate and sodium remain roughly constant depending only on atmospheric concentrations. Increases observed in snow concentrations with decreasing snow accumulation are explained by the increasing relative contribution of dry deposition flux. This effect is expected to be particularly important at more central sites, where dry deposition may account for 80% or more of snow content. The conclusion of Legrand (1995) and de Angelis et al. (1997) may be valid for other non-reversible aerosol-like wind-borne dust but not likely for species with different physico-chemical properties, such as reactive gases or reversible salts. Nevertheless, and despite the noise introduced in data interpretation by the reconstruction of past accumulation rates, deposition fluxes are often considered to be better suited to reconstruct atmospheric changes than snow concentrations at sites where the

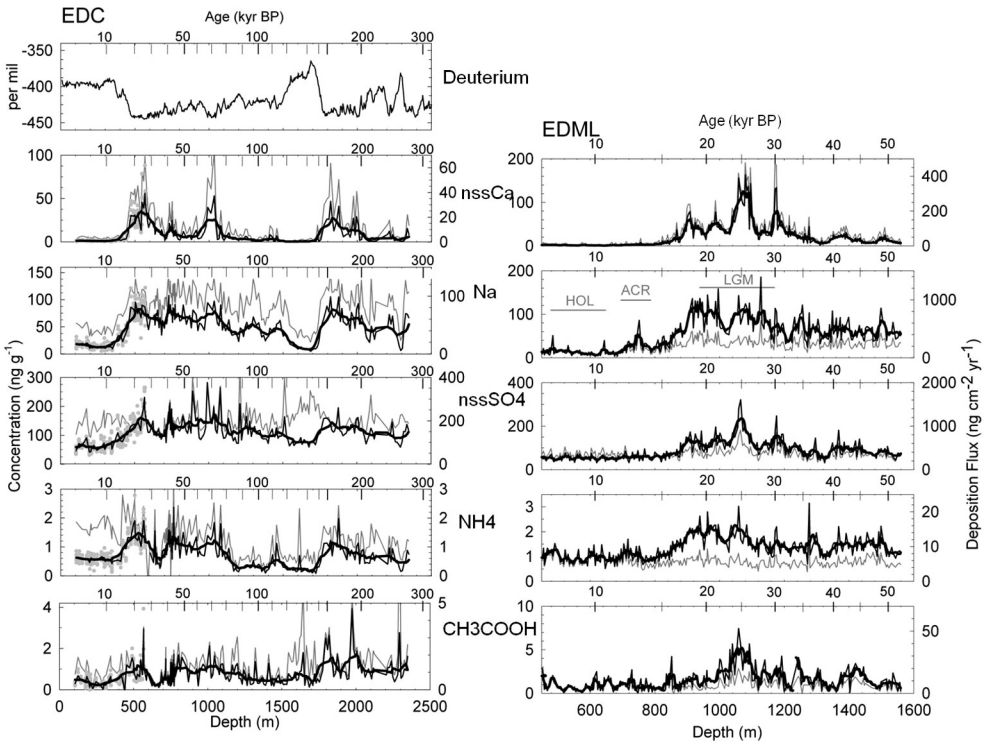

Fig. 3. EDC (left) and EDML (right) depth profiles of nss calcium, sodium, nss sulphate, ammonium and acetate. Concentrations are expressed in $\mathrm{ng\,g^{-1}}$ (left axes) and deposition fluxes are expressed in $\mathrm{ng\,cm^{-2}\,yr^{-1}}$ (right axes). EDC: grey dots correspond to concentrations measured in samples from chemistry strips (see text), thin black lines (grey lines) correspond to mean concentrations (deposition fluxes) calculated for every chemistry strip and to concentrations (deposition fluxes) measured in samples from central lamellae and thick black lines correspond to five samples concentration running means. EDML: thin black (grey) lines indicate concentrations (deposition fluxes) and thick black lines indicate the five samples concentration running means. The climate reference along EDC is given by the deuterium profile (top) and the age scale is indicated on the graphs' upper axes. The main climate stages recorded along EDML are indicated on the sodium graph and the age scale is indicated on the graphs' upper axes.

accumulation rate is low and is expected to have significantly changed with climate conditions, which is the case here. Deposition fluxes expressed in $\mathrm{ng\,cm^{-2}\,yr^{-1}}$ (right axes) are indicated by grey lines in the corresponding concentration panels of Fig. 3.

Additional information could be provided by inter-ion relationships using selected source markers. However, given that the time period covered by individual samples (4–8 yr) and the discontinuous sampling allow to investigate only long-term changes in atmospheric patterns, sporadic events of short duration likely to significantly disturb pluriannual mean concentrations should be removed. Sporadic events of global importance commonly identified in Antarctic ice cores correspond to stratospheric fallout from major volcanic eruptions. During such events, the sulphate volcanic component, which represents $<10\%$ of the total sulphate deposited over Antarctica during background periods (Cosme et al., 2005), significantly increases. Thus, particular attention was paid to nss sulphate, which was considered to be a good proxy of DMS production by phytoplankton only once samples suspected to contain significant volcanic debris had been discarded. For that, we used the ionic balance H^+ [$H^+ = \Sigma$ (anion) $- \Sigma$ (cation)], where (anion) [(cation)] represents the concentration of every anion (cation) expressed in $\mu\mathrm{Eq\,l^{-1}}$). It has been demonstrated that H^+ corresponds to sample acidity provided that it remains positive. H^+ mean values (H^+_{mean}) and corresponding SDs were calculated for the whole set of data along every core. When the ionic balance was higher than ($H^+_{\mathrm{mean}} + 2 * \mathrm{SD}$), that is, in samples corresponding to acidity outliers, the acidity was always counterbalanced by sulphate indicating the presence of large amounts of H_2SO_4 very likely of volcanic origin. The corresponding data were discarded. Ammonium and acetate concentrations are indicated as functions of nss sulphate, sodium and nss calcium (acetate only) concentrations for Holocene and last glacial maximum (LGM) time periods in the left part of Fig. 4 for EDC and in the right part for EDML.

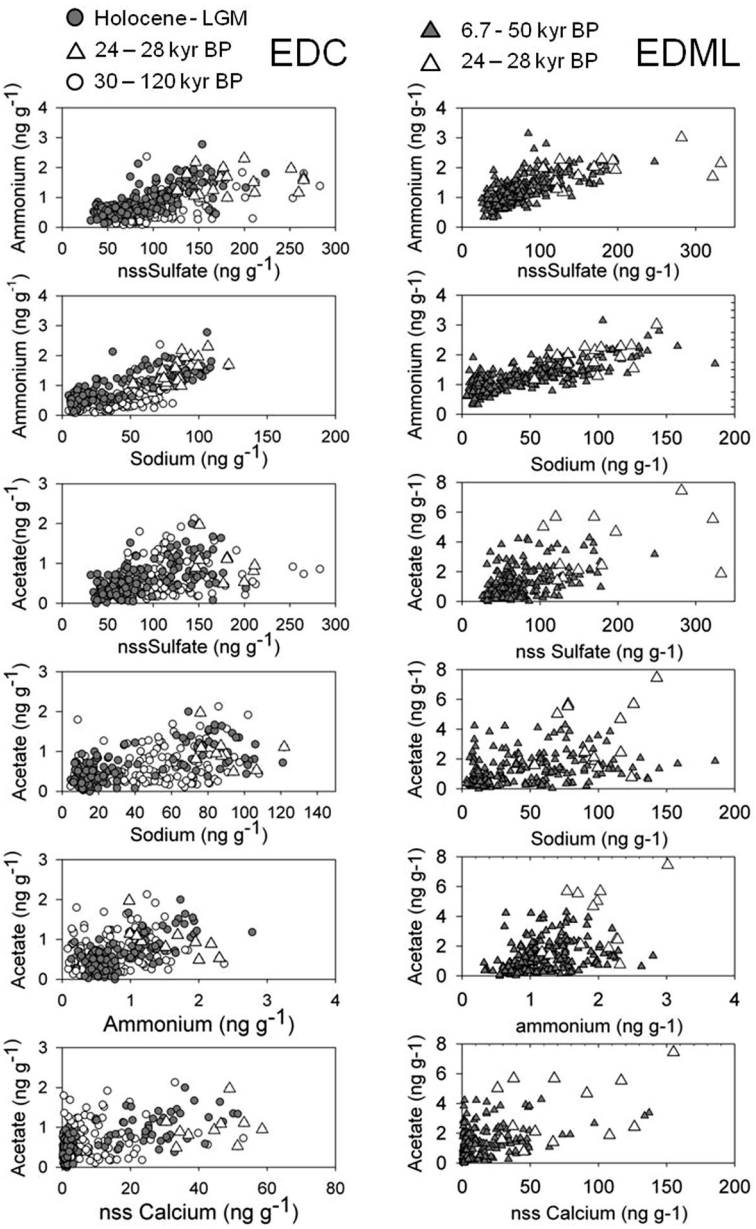

Fig. 4. Inter-species relationships (concentrations are expressed in ng g^{-1}). From top to bottom: ammonium as a function of nss sulphate, ammonium as a function of sodium, acetate as a function of nss sulphate, acetate as a function of sodium, acetate as a function of ammonium and acetate as a function of nss calcium. EDC (left part): grey circles and white triangles correspond to the past 30 kyr (Holocene and LGM, samples reprocessed in 2001 and 2002), white triangles cover the 24–26.5 kyr BP time period (see text) and white circles correspond to the remaining part of the last climatic cycle (30–120 kyr BP, samples reprocessed in 2003 and 2006). EDML (right part): white triangles correspond to 24–28 kyr BP (see text) and grey triangles correspond to the remaining part of the past 50 kyr.

Acetate, formate, nitrate, sodium, nss calcium and nss sulphate mean concentrations and deposition fluxes calculated for selected time periods discussed in the next two sections are indicated in Table 2.

3.2.1. Acetate in EDC. As shown in Fig. 3 and Table 2, acetate concentrations were higher during a large part of the last two glacial periods than under milder climate conditions (penultimate interglacial period and Holocene). Despite the noise induced by slight differences in analytical conditions between the different sets of data and by the rather large scattering of acetate blank values, a relatively clear pattern is visible over the last climatic cycle: acetate concentrations did not significantly change during the first part of the last glacial period (115–85 kyr BP), with a mean value close to

Table 2. Mean concentrations/deposition fluxes and corresponding SDs of acetate, formate, nitrate, sodium, ammonium, nss sulphate and nss calcium calculated along selected sections of EDC and EDML ice cores (see Section 3.2)

	Acetate	Formate	Nitrate	Sodium	Ammonium	Nss calcium	Nss sulphate
EDC							
Concentrations ($ng\,g^{-1}$)							
Penultimate interglacial	0.62±0.41	0.25±0.16	19±6	9.8±2.8	0.20±0.14	0.47±0.14	75±8
115–85 kyr BP	0.50±0.32	0.18±0.07	12±7	46±12	0.38±0.21	2.7±2.2	108±22
85–30 kyr BP	0.76±0.48	0.21±0.08	16±9	65±18	0.93±0.44	11±10	130±43
LGM, 28–24 kyr BP (1)	1.0±0.5	0.22±0.13	36±13	81±17	1.4±0.4	32±14	149±42
LGM, 30–25 and 23–18 kyr BP (2)	1.3±0.8	0.26±0.14	44±18	87±15	1.5±0.4	45±15	189±49
LGM, 30–18 kyr BP	0.94±0.38	0.19±0.12	32±9	79±17	1.4±0.4	26±9	132±22
Holocene	0.32 ± 0.24	0.22±0.14	10±2	14±5	0.57±0.14	1.10±0.46	60±19
Deposition fluxes ($ng\,cm^{-2}\,yr^{-1}$)							
Penultimate interglacial	2.1±1.3	0.89±0.59	69±28	34±7	0.70±0.48	1.7±0.6	264±40
115–85 kyr BP	0.89±0.53	0.33±0.14	23±14	85±20	0.7±0.4	4.8±3.5	200±37
85–30 kyr BP	1.2±0.8	0.33±0.13	24±12	98±20	1.4±0.6	16±13	198±64
LGM, 28–24 kyr BP (1)	1.3±0.7	0.28±0.17	47±17	106±22	1.8±0.6	42±18	195±52
LGM, 30–25 and 23–18 kyr BP (2)	1.6±1.2	0.28±0.14	57±24	109±20	2.0±0.5	58±17	252±63
LGM, 30–18 kyr BP	1.2±0.5	0.26±0.16	43±13	105±24	1.8±0.6	35±12	175±32
Holocene	0.92±0.68	0.66±0.44	31±7	43±15	1.7±0.4	3.4±1.3	182±57
EDML							
Concentrations ($ng\,g^{-1}$)							
55–35 kyr BP	1.5±1.0	0.55±0.24	47±6	61±22	1.4±0.4	15±9	53±10
LGM, 30–18 kyr BP	2.6±1.6	0.22±0.14	75±35	89±29	1.7±0.4	56±39	137±49
LGM, 28–24 kyr BP (1)	4.3±1.9	0.27±0.14	116±41	102±20	1.9±0.4	104±39	187±54
LGM, 30–25 and 23–18 kyr BP (2)	2.1±1.2	0.21±0.13	63±20	84±30	1.7±0.4	41±24	122±35
Holocene	0.86±0.67	0.55±0.24	47±6	13±8	0.97± 0.25	1.5±0.6	53±10
Deposition fluxes ($ng\,cm^{-2}\,yr^{-1}$)							
55–35 kyr BP	5.8±3.8	0.56±0.31	230±51	240±79	5.4±1.4	59±34	327±88
LGM, 30–18 kyr BP	8.2±3.4	0.71±1.05	243±68	286±112	5.5±1.3	179±63	444±99
LGM, 28–24 kyr BP (1)	12.7±5.7	0.81±0.39	346±122	308±57	5.6±1.2	308±113	557±148
LGM, 30–25 and 23–18 kyr BP (2)	6.9±3.9	0.68±0.42	211±64	279±99	5.5±1.3	139±85	408±125
Holocene	5.7±4.4	3.63±1.54	313±47	85±50	6.4±1.6	9.9±4.1	351±73

Concentrations and deposition fluxes are given in $ng\,g^{-1}$ and in $ng\,cm^{-2}\,yr^{-1}$, respectively. LGM (1) corresponds to the part of the LGM when very high concentrations of acetate, nitrate and nss calcium are observed in EDML (see text) and LGM (2) corresponds to the remaining part of the LGM.

the mean value calculated for the penultimate interglacial period. Then they increased and, except a marked minima centred at 33 kyr BP, they remained high from ca. 85 kyr BP to the end of the LGM (18–30 kyr BP), showing three broad relative maxima of the same amplitude. They decreased during the last climatic transition to reach a mean Holocene value approximately three times lower than the mean value calculated for the LGM. Two broad relative maxima may be observed between the end of the penultimate interglacial period and 85 kyr BP in sodium, nss sulphate and ammonium profiles, superimposed by a background of increasing trend of sodium and nss sulphate concentrations, which are more pronounced for sodium. Mean concentrations calculated for the 115–85 kyr BP time period are higher than mean concentrations corresponding to the penultimate interglacial period. The difference is moderate for nss sulphate (increase by a factor of 1.3). Higher increases are observed for sodium and ammonium with mean concentrations, four and two times higher, respectively, over the 115–85 kyr time period than over the penultimate interglacial period. Non-sea-salt sulphate, sodium and ammonium concentrations remained high from 85 kyr BP to the end of the LGM, except the broad minimum centred at 33 kyr BP and previously observed on the acetate profile, which is visible only on the ammonium profile. The relative minimum centred at 55 kyr BP on the acetate profile is also visible on the ammonium and sodium profiles. LGM mean values are 2.5, 2.5 and 6 times higher than Holocene corresponding mean values for nss sulphate, ammonium and sodium, respectively.

Inter-ion relationships are shown in Fig. 4, where white circles correspond to the last climatic cycle (past 120 kyr) and grey circles to the past 30 kyr. White triangles correspond to 28–24 kyr BP, the time when a large continental event is registered in EDML. As is expected from similarities in background trends observed in Fig. 3, ammonium is well correlated with sodium ($r = 0.74$) and nss sulphate ($r = 0.62$) over the past 120 kyr. The correlation is even better over the past 30 kyr ($r = 0.85$ and $r = 0.74$ with sodium and nss sulphate, respectively). The correlation of ammonium with nss sulphate weakens only around ca. 25 kyr BP, when nss sulphate increases by a factor close to 2. As ammonium acetate appears to be significantly correlated with sodium ($r = 0.50$) and nss sulphate ($r = 0.44$) over the past 120 kyr and correlations are better over the past 30 kyr ($r = 0.61$and $r = 0.59$, with sodium and nss sulphate, respectively). Acetate and ammonium are significantly correlated over the whole climatic cycle ($r = 0.46$) and the past 30 kyr ($r = 0.59$). Differences in background trends during the first part of the last glacial age combined for acetate with higher analytical noise (see Section 2) may explain that correlations are better when only samples covering the past 30 kyr are taken into account. Acetate is also significantly correlated with nss calcium. The correlation is better over the past 30 kyr ($r = 0.74$) than over the past 120 kyr ($r = 0.57$) and is driven by the coincidence of rather high acetate concentrations with nss calcium peaks during glacial extrema centred at 25 and 70 kyr BP (see Fig. 3). However, large differences in acetate and nss calcium concentration trends are visible in Fig. 3 and Table 2: (1) the progressive increase of nss calcium observed from the beginning of the last glacial period until 80 kyr BP (from 0.5 to 4 ng g^{-1}) is quite moderate and of low amplitude compared with peak values (ca. 60 ng g^{-1}), which is not true for acetate; (2) calcium concentrations remain relatively low from 60 to 40 kyr BP, whereas a broad peak is visible on acetate depth profile.

Snow accumulation rates were lower under glacial conditions than during the Holocene, which implies that the wet component of aerosol deposition fluxes should have remained very low over Dome C compared with the dry one over the whole glacial cycle. This conclusion makes it relevant to use changes in deposition fluxes to investigate corresponding changes in atmospheric composition over the past 120 kyr (Legrand, 1995; de Angelis et al., 1997). The Southern Ocean was most likely the prominent source not only of sodium and nss sulphate but also of ammonium for the interior of Antarctica during the past (Kaufmann et al., 2010). As shown in Table 2 and visible in Fig. 3, the ammonium deposition flux increased by a factor close to three between the 115–85 kyr BP time period and the LGM and slightly decreased (by approximately 10%) during the last climatic transition. The sodium deposition flux followed a similar trend, starting to increase at the beginning of the last glacial period and remaining high until the beginning of the transition. The Holocene mean deposition flux was 2.5 times lower than during the LGM. On the contrary, the nss sulphate deposition flux remained more or less constant over the whole climatic cycle. The acetate deposition flux slightly increased during the last glacial age and decreased during the last climatic transition, which suggests that acetate (as non-reversible salt) atmospheric content was higher during the second half of the glacial age than during the Holocene, following sodium and ammonium rather than nss sulphate atmospheric load.

Taken together, trend comparison and inter-ion relationships lead us to conclude that the mechanisms proposed for the formation of acetic acid in the present Antarctic atmosphere (Legrand et al., 2004) and acetate deposition at Dome C under present climate conditions are consistent with the main features of EDC data over the past 300 kyr. That is to say that the production of acetic acid in the Antarctic atmosphere is directly related to the marine biogenic activity: in winter, the photochemical degradation of dissolved organic carbon released by phytoplankton produces alkenes and is followed by ozone – alkene reactions; in summer, acetate could come from peroxy acetyl radicals formed after successive reactions in a gaseous phase initially involving propene. Such mechanisms may explain the relationship observed with ammonium through ammonia consumption and regeneration by phyto- and zoo-plankton in the Southern Ocean (Atkinson and Whitehouse, 2001), and the correlation with nss sulphate. Increased cyclonic activity and transport efficiency over the Southern ocean during the glacial age is probably partly responsible for the relationship with marine primary aerosol, which was likely improved by the uptake of sea-salt particles during transport (Matsumoto et al., 1998). However, heterogeneous reactions at the surface of wind-borne dust may have acted as an additional sink of acetic acid of marine or more likely continental origin under full glacial conditions as discussed in the following section.

3.2.2. Acetate in EDML. Sodium and ammonium patterns in EDML are roughly the same as in EDC. Sodium (ammonium) mean concentration increases by a factor of 1.5 (1.2) between the deeper part of the core covering from 55 to 35 kyr BP and the part of the core corresponding to the LGM (30–18 kyr BP), and then decreases by a factor of 6.8 (1.9) to reach the Holocene plateau. Ammonium is well correlated with sodium ($r = 0.78$). The correlation with nss sulphate is a bit weaker ($r = 0.69$) and also weaker than along EDC for the same time period, particularly for lower concentrations. As shown in Table 2, the significant

differences with EDC are observed mainly during the LGM for acetate, nss calcium, nitrate and nss sulphate. Acetate mean concentration roughly increases by a factor of two between the 55–35 kyr BP time period and the LGM (30–18 kyr BP) and then decreases by a factor of three during the last transition. However, acetate concentrations significantly higher than elsewhere during the LGM are observed from 1040 to 1100 m deep, i.e. between 24 and 28 kyr BP (marked LGM (1) in Table 2). They coincide with a very high peak of nss calcium, where concentrations reach values as high as 150 ng g^{-1} and a more moderate peak of nss sulphate. Acetate (nss sulphate) mean concentration over the 1040–1100 m depth interval is more than two (1.5) times higher than the LGM mean concentration calculated after samples corresponding to the peak have been removed (set of samples marked LGM (2) in Table 2). Concentrations of nss calcium as high as those found in EDML around 26 kyr BP have never been observed on the central plateau, neither at Dome C nor at Vostok in samples with similar time resolution (i.e. several years, see for instance de Angelis et al., 1992 or Legrand and Mayewsky, 1997). The nss calcium mean value calculated for the 24–28 kyr BP time period is more than two times higher in EDML than in EDC. A focus on this particular event is made in Fig. 5, where concentration profiles of nitrate (Fig. 5a, grey line of the lower graph), nss calcium (Fig. 5a, black line of the lower graph) and acetate (Fig. 5b) are indicated along with ionic balance (Fig. 5a, black line of the upper graph where corresponding values are expressed in μEq l^{-1} on the right scale). The very high concentrations of nss calcium observed around 26 kyr BP are associated with unusually low and sometimes negative values of the ionic balance. The mean value of the ionic balance calculated for the 24–28 kyr BP time period (0.4 ± 1.6 μEq l^{-1}) is significantly lower than at Dome C for the same period (1.8 ± 0.5 μEq l^{-1}) and this denotes the arrival of very large amounts of alkaline dust at Kohnen Station at that time. A moderate peak is also observed for nss sulphate, whereas sodium and ammonium concentrations do not show a similar increase (see Fig. 3). This likely explains the much weaker correlations observed between acetate and ammonium ($r = 0.35$) or sodium ($r = 0.35$) along EDML, though analytical conditions made it possible to get a more homogeneous dataset than along EDC. On the other hand, a common trend seems to still exist with nss sulphate ($r = 0.53$).

The question why higher acetate concentrations are associated with unusually high amounts of mineral dust in EDML is open.

As shown in Fig. 6 (lower part), a good linear correlation between nss calcium and nss sulphate deposition fluxes is observed over the past 55 kyr ($r = 0.63$). The correlation is even better during the LGM ($r = 0.72$). Moreover, the slope of the nss calcium – nss sulphate regression line is 0.49 for

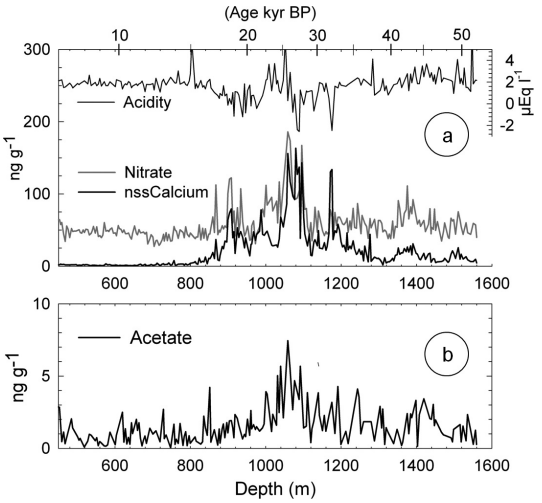

Fig. 5. (a) From top to bottom: EDML depth profiles of ionic balance H+ (black line, right axis), nitrate (grey line, left axis) and nss calcium (black line, left axis); (b) EDML concentration depth profile of acetate. Ionic balance is expressed in μEq l^{-1}. Concentrations are expressed in ng g^{-1}.

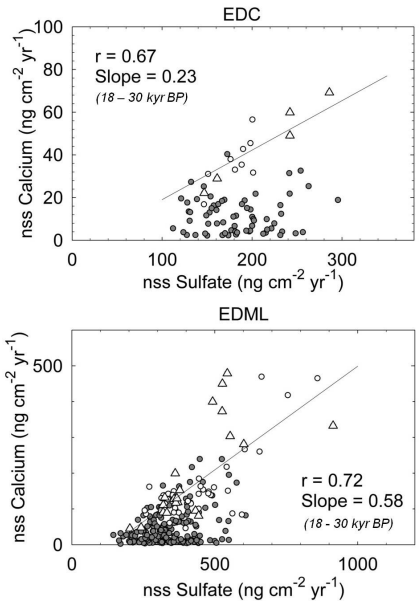

Fig. 6. Relationships between non-sea-salt calcium and non-sea-salt sulphate deposition fluxes along EDC (top – mean deposition fluxes, when corresponding to chemistry strips) and EDML (bottom) for the past 55 kyr. White dots and white triangles correspond to the LGM (18–30 kyr BP), white triangles cover the 24–28 kyr BP time period (see text) and grey dots correspond to the remaining part of the samples. Linear regression lines and correlation coefficients corresponding to the LGM are also indicated; deposition fluxes are expressed in ng cm^{-2} yr^{-1}.

samples covering the past 55 kyr and 0.58, when only samples covering the LGM are taken into account. These values are close to or higher than the slope corresponding to stoichiometric equilibrium (0.42). This strongly suggests that nss sulphate was present as primary or secondary gypsum and tightly associated with continental dust over the EDML during the glacial age. Significant amounts of secondary gypsum resulting from heterogeneous reactions between gaseous SO_2 and wind-borne mineral particles have been observed in aerosol from remote marine or continental sites, where mineral particles are internally mixed with atmospheric acids (Andreae et al., 1986; Winchester and Wang, 1989). In addition, ice core studies have provided the evidence of very efficient neutralisation processes taking place in the South American atmosphere between calcium-containing particles and SO_2 emitted by Andean volcanoes and/or biomass burning leading to gypsum formation (de Angelis et al., 2003; Moreno Rivadeneira, 2011). Large amounts of carbonate-rich particles transported at rather low altitude over the Southern Atlantic Ocean during the glacial age (and particularly the large event centred at 26 kyr BP) may have provided sites for the heterogeneous oxidation of marine biogenic SO_2 formed in the marine boundary layer or the lowermost free troposphere (Piel et al., 2006; Andreae et al., 1986) and entrapped acetic acid of marine origin at their surface. However, this explanation is not convincing because methane sulphonic acid (not shown here), which is another abundant acid of marine biogenic origin should also have been partly involved in reactions at the surface of dust particles, which is not the case. Moreover, only a partial neutralisation of clay or carbonate particles is observed in the present marine atmosphere even in areas where SO_2 concentrations are greatly increased by volcanic contribution (Gao et al., 2007): since the concentration of marine biogenic SO_2 over the Southern Ocean is not expected to have significantly increased in the past (Fischer et al., 2007), a complete neutralisation of greater amounts of carbonate dust by marine biogenic SO_2 under glacial conditions may hardly be evoked to explain the relationship linking nss calcium and nss sulphate in EDML.

Further information may be inferred from the nitrate concentration profile. In EDML, the nitrate mean concentration corresponding to the event at 24–28 kyr BP is two times higher than during the remaining part of the LGM, 2.5 times higher than during the Holocene and more than three times higher than in EDC for the same period. As shown in Fig. 5a, nitrate is tightly related to nss calcium. Despite lower snow accumulation rates, large increases of nitrate concentrations coinciding with high mineral dust content have been observed for a long time in glacial ice of central Antarctic sites experiencing strong post-deposition losses (e.g. Legrand et al., 1988; Röthlisberger et al., 2000). Authors concluded that this may reflect efficient scavenging of HNO_3 by dust particles preventing its post-depositional loss. Given the efficiency of HNO_3 (and/or NO_x) adsorption and its subsequent conversion to nitrate on the surface of mineral dust (Ooki and Uematsu, 2005; Kim and Park, 2001; Pretzler Prince et al., 2008), it is clear that the part of atmospheric nitrate entrapped in snow archives was stuck at the surface of mineral particles at times of large wind-borne dust input. However, sticking may have occurred very close to production areas if nitrate is of continental origin, during transport through air mass exchanges or within the firn layer. Several reasons lead to discard post-depositional sticking processes as the one and only cause of nitrate peaks observed in the glacial part of Antarctic ice cores: (1) numerous Vostok ice samples deposited during the glacial age contain nitrate concentrations similar to those observed in interglacial ice in spite of significantly higher nss calcium levels (Legrand et al., 1999); (2) nitrate does not increase in the snow layer containing Cerro Hudson deposits in the Dome C pit (see Section 3.1); whatever the origin of nitrate in recent Antarctic snow, this tends to demonstrate that mineral dust once deposited does not significantly capture reactive nitrogen species remobilised within firn; (3) a comprehensive study of the nitrogen and oxygen isotopic composition of nitrate performed along the Vostok ice core suggests that post-depositional processes leading to nitrate losses at the snow surface have not ceased during the last glacial period in spite of the presence of large amounts of mineral dust (Erbland et al., 2009a) and that oxidation pathways of nitrate entrapped in the ice archive may have been different and more influenced by heterogeneous chemistry at that time (Erbland et al., 2009b). Referring to EDML data, it must be noted that: (1) while only approximately 30% of nitrate is released from the Kohnen Station snow surface under present climate conditions (Weller et al., 2004), nitrate concentrations higher than 180 ng g^{-1} (i.e. almost four times higher than the Holocene mean value) are found around 26 kyr in EDML; (2) without any significant difference in atmospheric load over the EDML and the central EDC, nitrate concentrations should be fairly similar in EDML and EDC ice sections where large dust inputs are observed, which is obviously not the case as shown in Table 2. Taken together, all these observations support the hypothesis of higher atmospheric concentrations of HNO_3 (and/or NO_x) over the EDML during the glacial age than: (1) under present climate conditions and (2) over the Dome C area during the glacial age. They also strongly suggest that the origin and/or transport pathways of nitrogen species were different during the glacial age, when nitrate was associated with nss calcium: in particular, HNO_3 (and/or NO_x) emitted by continental sources and uptaken at the

surface of carbonate-rich particles close to the source areas may have been transported towards the EDML.

Consequently, we propose that more efficient transport processes from continental areas around 26 kyr BP could have provided the DML sector with well-mixed air masses containing not only mineral particles but also species emitted from soils, tropospheric volcanism, vegetation and likely burning events, among them acetate and nitrate. The synergistic effect observed between nitric and acetic acids in uptake experiments at the surface of calcite aerosol under ambient conditions by Pretzler Prince et al. (2008) supports the hypothesis of common source regions for nss calcium, nitrate and acetate at that time. Compared with the composition of biomass burning deposits observed over the Patagonian ice cap (Vimeux et al., 2008; Moreno Rivadeneira, 2011), the absence of a clear corresponding trend of ammonium concentrations in EDML ice suggests that acetate and nitrate may come from vegetation and soil emissions rather than from biomass burning or that fire types in Patagonia were more of the flaming type during the glacial age than under present climate conditions (Savarino and Legrand, 1998).

Although significantly lower than in EDML, nitrate, acetate, nss calcium and nss sulphate concentrations also increased around 26 kyr BP in EDC (Table 2). As shown in Fig. 4 (white triangles), the ammonium – nss sulphate correlation weakens at this time and scattered and sometimes high acetate concentrations are associated with nss calcium concentrations among the highest of the whole climatic cycle. In other EDC panels, particularly those involving acetate, the time period centred at 26 kyr BP cannot be clearly distinguished from the rest of the climatic cycle. While nss sulphate and nss calcium deposition fluxes are not correlated over the past 55 kyr ($r = 0.22$), a good correlation, although weaker than in EDML, is observed during the LGM ($r = 0.67$, Fig. 6, upper panel). However, the slope of the nss calcium – nss sulphate regression line calculated for LGM samples is 0.23, almost twice as low as expected from stoichiometric equilibrium. All this suggests that continental air masses that strongly and regularly impacted the EDML from 28 to 24 kyr BP were markedly depleted or diluted by polar or marine air before reaching the EDC, where the budget of acetate and nss sulphate remained largely influenced by marine input outside of sporadic continental events.

3.3. Formate

Concentration depth profiles of formate along EDC (left) and EDML (right) are shown in Fig. 7 along with corresponding methane profiles (Loulergue et al., 2008; EPICA Community Members, 2006). Climate trends at both sites are tracked by deuterium (EDC) and sodium (EDML) profiles. The lowest formate concentrations along EDC are found at the onset of the last glacial age ($0.12 \pm 0.05\,ng\,g^{-1}$ from 120 to 110 kyr BP). Later, formate concentrations progressively increase and values roughly two times higher ($0.22 \pm 0.07\,ng\,g^{-1}$) are found from 90 to 40 kyr BP. After a marked decrease at 30–35 kyr BP ($0.12 \pm 0.05\,ng\,g^{-1}$), they increase again at the end of the glacial age and remain high during the Holocene. Data scattering is significantly higher in core sections, including the Holocene ($0.23 \pm 0.15\,ng\,g^{-1}$), the last transition and the penultimate interglacial period ($0.26 \pm 0.14\,ng\,g^{-1}$). This observation is also valid along EDML over the past 52 kyr: formate concentrations are low between 52 and 28 kyr BP ($0.14 \pm 0.08\,ng\,g^{-1}$). A first increase is observed during the LGM (28–17.5 kyr BP) with a mean value of $0.22 \pm 0.13\,ng\,g^{-1}$ followed by a second increase at the end of the glacial period with a mean value of $0.54 \pm 0.23\,ng\,g^{-1}$ for the 15–6.5 kyr BP time period. As in EDC, higher scattering is observed during the past climatic transition and the Holocene. Interestingly, a rather similar trend is observed in ice from the edge of the EDC (D10 ice core see Section 3.1) with formate concentrations also less scattered during glacial periods ($0.2 \pm 0.1\,ng\,g^{-1}$) than during the Holocene ($1.4 \pm 0.7\,ng\,g^{-1}$). Furthermore, the formate concentration range in the glacial part of the D10 core is close to what we found at both EPICA sites under glacial conditions.

Glacial age accumulation rates at Kohnen Station were more than two times higher than at Dome C, that is, even higher than during the Holocene. Similarly, we may expect glacial snow accumulation rates on the border of the EDC in the same range as EDML Holocene values, that is, higher than at Dome C, whatever the climate stage. This led to correlating the similarities in formate concentrations observed along the three cores under glacial conditions to homogeneous atmospheric content over a large part of East Antarctica at that time rather than to large-scale post-deposition losses.

Although lower concentrations during the glacial age are also observed for methane, the time when methane concentrations are minimum (LGM) corresponds to the first increase of formate concentrations in EDML and the overall increase of methane from glacial to temperate conditions is close to 1.8 when it is higher than 4 for formate in EDML. This led to the conclusion that methane oxidation through formaldehyde in cloud oxidation is not the major source of formate deposited in Antarctica.

For now, and contrary to acetate, the oxidation of alkenes by ozone can explain only the winter levels of formic acid and another mechanism involving formaldehyde is required for summer levels. Besides CH_4 oxidation, an additional photochemical mechanism has to be considered to explain the high formaldehyde mixing ratios

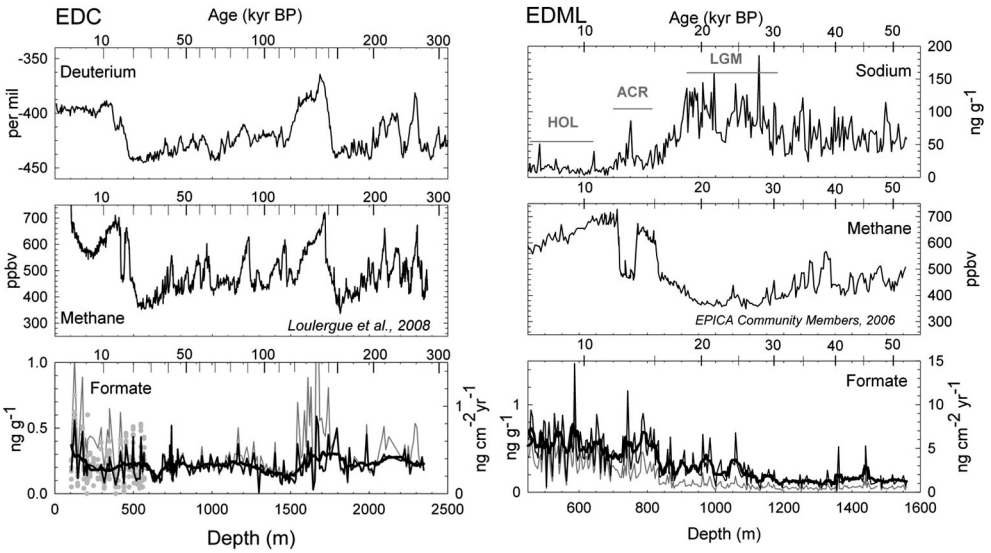

Fig. 7. EDC (left) and EDML (right) depth profiles of formate. Concentrations are expressed in ng g^{-1} (left axes) and deposition fluxes are expressed in ng cm^{-2} yr^{-1} (right axes). EDC: grey dots correspond to concentrations measured in samples from chemistry strips (see text), thin black lines (grey lines) correspond to mean concentrations (deposition fluxes) calculated for every chemistry strip and to concentrations (deposition fluxes) measured in samples from central lamellae and thick black lines correspond to five samples concentration running means. EDML: thin black (grey) lines indicate concentrations (deposition fluxes) and thick black lines indicate the five samples concentration running means. The climate reference along EDC is given by the deuterium profile (top) and the age scale is indicated on the graphs' upper axes. The main climate stages recorded along EDML are indicated on the sodium graph and the age scale is indicated on the graphs' upper axes.

observed at high Southern latitudes. However, the corresponding steady-state mixing ratio of formic acid does not account for the concentrations observed and another yet unknown source is needed (Legrand et al., 2004; Paulot et al., 2011). Based on the discussion of EDC acetate profiles, we may expect a greater contribution of alkene oxidation to the production of mono-carboxylic acids (factor of about two) during the glacial age than under milder climate conditions. As shown in Fig. 7, formate concentrations tend to be lower under glacial than under interglacial conditions. However, formate and acetate trends in EDC are similar between 440 and 880 m, that is, from 50 to 16 kyr BP, showing a marked minimum centred at 33 kyr BP and flanked by two broad peaks (see also Fig. 3). Assuming that uptake on marine aerosol was of similar efficiency for both species, this suggests that the role played by alkene oxidation on formate production did not drastically weaken under glacial conditions but that the relative importance of the additional production from formaldehyde and by the unknown source evoked by Legrand et al. (2004) markedly decreased during the glacial age, allowing the part represented by methane oxidation to increase. Staffelbach et al. (1991) observed a strong decrease of formaldehyde along the Byrd core (Western Antarctica) during the glacial age, with minimum values more than 20 times lower than Holocene values during the LGM. This supports the hypothesis of the weakening of formate production by extra-methane formaldehyde sources. Changes in the CH_4/HCHO ratio along the Byrd core were discussed in terms of possible OH depletion during the glacial age, which in turn should have contributed to reduce the formate production by methane oxidation. This effect may have been counterbalanced by the increasing influence of the unknown source proposed by Legrand et al. (2004) after 30 kyr BP.

Acetate to formate ratios in the range of present atmospheric values over polar areas are found only in core sections covering interglacial stages (see Tables 1 and 2). Higher ratios are observed during the glacial age with values close to 4 along EDC and higher than 10 along EDML. As discussed in Section 3.2, heterogeneous uptake on alkaline aerosol of marine or continental origin was very likely a significant sink for acetic acid during the glacial age, particularly at EDML in association with nitric acid at the time of major arrival of carbonate-rich particles. As we may expect a similar influence of ambient temperature and relative humidity on uptake kinetics for acetic and formic acids (Pretzler Prince et al., 2008; Al-Hosney et al., 2005; Hatch et al., 2007), the increase of acetate to formate ratio observed during the glacial age must be rather related to the decreasing influence of part of the present sources of formic acid combined with an additional acetate source

during the LGM: interaction between fresh biomass burning plumes (Keene et al., 2006; Paulot et al., 2011) and soil dust remobilised by strong convection during fire events or wind-borne dust from semi-arid Patagonian areas could, for instance, explain the absence of major formate increase around 26 kyr BP (0.27 ± 0.14 ng g^{-1}).

3.4. *Comparison with other sites – present climate conditions*

An attempt to better understand the geographical variability of mono-carboxylate under temperate climate conditions was made by comparing EDC and EDML mean Holocene concentrations and SDs with data from other remote sites in Greenland (Dome Summit), South America (San Valentin) and Antarctica (D10, Berkner Island, Talos Dome and Vostok). Data are shown in Table 3. Antarctic sites used for the comparison are indicated on the Antarctic map in Fig. 8. The San Valentin firn core is a shallow core covering the 1964–2005 time period, but human activity at this site was strictly restricted to a very short drilling operation with solar power supply. Thus, we consider that San Valentin concentrations provide a valuable estimate of natural Patagonian background values. Formate and acetate were measured back to 1930 along a firn core recovered at GD09, in the Wilkes Land, which is also a well-preserved site. However, this core was stored in polyethylene bags for several years. For that reason, the corresponding data are not shown in Table 3. San Valentin and Dome Summit mean values and SDs were calculated after removing large biomass burning events.

Formate and acetate concentrations are one order of magnitude lower in Antarctic ice than in ice from other sites. This is puzzling as atmospheric concentrations are in the same range at Dome Summit, Dumont D'Urville and South Pole, and raises again the question of the incorporation of gaseous species to polar precipitation. As discussed in Section 3, reactive uptake of aerosol seems to be a significant sink of formic and acetic acids over the Antarctic ice cap. However, two points must be underlined: (1) Dibb and Arsenault (2002) suggested that oxidation of carbonyls and alkene (produced by photo- and OH-oxidation of ubiquitous organic compounds) within the snow pack may be a source of mono-carboxylic acids for the air aloft and

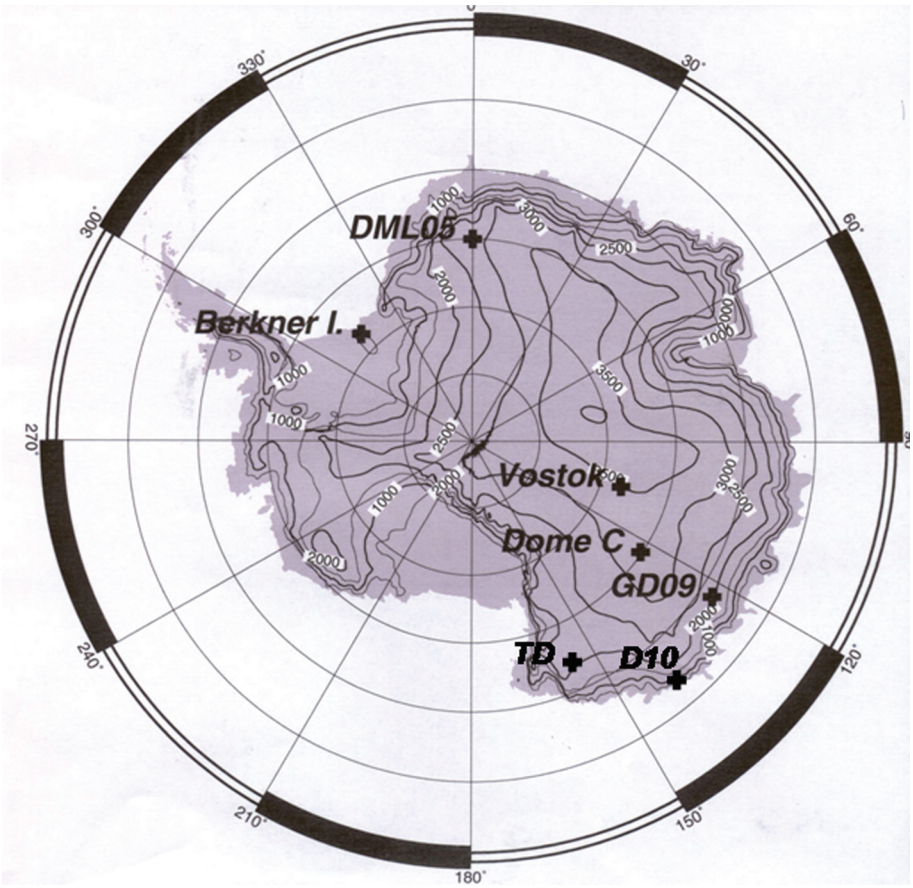

Fig. 8. Antarctic map showing the location of sites shown in Table 3.

Table 3. Comparison of EDC and EDML Holocene mean concentrations of acetate, formate, oxalate, ammonium, nitrate and sodium with concentrations measured in firn and ice layers of other remote sites (corresponding SDs are in parentheses)

	Acc. Rate ($g\,cm^{-2}\,yr^{-1}$)	Acetate ($ng\,g^{-1}$)	Formate ($ng\,g^{-1}$)	Oxalate ($ng\,g^{-1}$)	Ammonium ($ng\,g^{-1}$)	Nitrate ($ng\,g^{-1}$)	Sodium ($ng\,g^{-1}$)
Dome Summit (Greenland)	23	9.3 (1.4)	10.7 (1)	0.6 (1.2)	4.5 (1)	62 (19)	6.2 (5.4)
San Valentin (Patagonia)		5.1 (0.5)	6.5 (5.5)	0.34 (1.15)	1.3 (2)	17 (5)	239 (27)
D10	19 (6)		1.4 (0.7)			49 (6)	12 (1)
Berkner Island	13	0.11 (0.09)	0.1 (0.08)	<0.1	1.9 (0.3)	34 (5)	594 (150)
Talos Dome	7.5	1.2 (1.6)	0.3 (0.33)	0.05 (0.09)	0.57 (0.39)	46 (12)	15 (17)
DML05	6.2	0.86 (0.67)	0.55 (0.24)	<0.01	0.9 (0.2)	47 (6)	13 (8)
DC	3.2	0.32 (0.24)	0.22 (0.14)	0.019 (0.03)	0.57 (0.14)	10 (2)	14 (5)
Vostok	2.2	0.16 (0.16)	0.16 (0.07)	0.2 (0.02)	0.74 (0.18)	11 (1)	17 (7)

Dome Summit data are from Legrand and de Angelis (1995) and Savarino and Legrand (1998). San Valentin data are from Vimeux et al. (2008). D10 data are from Legrand and de Angelis (1995) and Legrand (1985): concentration ranges correspond to the Holocene part of the core assumed to originate 300–400 km inland and the accumulation rate is deduced from present surface data measured 350–500 km from the coast along the DDU DC transect (Magand, personal communication). Other data are unpublished data from authors.

explain part of the very high mixing ratios observed; (2) the same geographical variability is observed for oxalate, which is expected to be in aerosol phase as for acetate and formate.

Although very preliminary, this study provides useful information. The influence of accumulation rate is not direct: either very low (Berkner Island, acetate and formate) or higher (D10, formate) concentrations are observed at sites, where accumulation rates are high (13 and $19\,g\,cm^{-2}\,yr^{-1}$ at Berkner Island and D10, respectively). The highest ammonium concentrations were found at Berkner Island, which is directly impacted by marine air masses as shown by very high sodium concentrations. This is not the case for acetate and could indicate that the acetate – sodium relationship observed at Dome C during the LGM-Holocene transition is only valid for air masses not directly transported from the ocean. In a general way, acetate concentrations seem to decrease with distance to open sea. On the contrary, no clear trend is visible for formate. This may indicate that the additional summer source expected to dominate the formate production under present climate conditions is rather homogeneously distributed around and over Antarctica. Further information on this unknown source should be inferred from its weakening during the glacial age in relation with sea ice formation and changes in oceanic circulation rather than biomass activity.

4. Conclusions

This study provides the first comprehensive investigation of formate and acetate present in Antarctic ice over time periods, including major climatic changes. Investigations were carried out along two deep ice cores recovered at two sites experiencing relatively different meteorological and glaciological conditions. This notably improves the data significance and interpretation. Reactive uptake on alkaline aerosol appears as a significant sink of formic and acetic acids in Antarctic atmosphere. The same trend is observed for formate over the central EDC and EDML: high and scattered concentrations observed during interglacial periods support the existence, in addition to alkene oxidation, of a major marine source providing most of formic acid under temperate climate conditions and rapidly weakening at interglacial – glacial transitions, the relative importance of formaldehyde and methane oxidation increasing under cold climate conditions. Geographical considerations suggest that the influence of this still unknown source of formic acid is rather homogeneous over a large part of Antarctica. Except the sporadic arrival of diluted continental plumes, the origin of acetate does not seem to have markedly changed over the Central EDC during the last two climatic cycles and remains linked with marine biomass activity. The significant increase of acetate observed in EDML from 28 to 24 kyr BP in the same time as large peaks of nitrate and gypsum-like material may indicate that emission from continental biomass was the major contributor to acetate budget at this time over the EDML. Passing from qualitative interpretation of deep ice core profiles to quantitative estimate of changes in past atmospheric composition now requires careful investigation of the air – snow transfer function.

5. Acknowledgements

This work is a contribution to EPICA, a joint European Science Foundation (ESF)/European Commission (EC)

scientific programme, funded by the EC (EPICA/MIS) and by national contributions from Belgium, Denmark, France, Germany, Italy, The Netherlands, Norway, Sweden, Switzerland and the UK. We thank all the personnel who have contributed to obtain ice core sampling.

References

Al-Hosney, H. A., Carlos-Cuellar, S., Baltrusaitis, J. and Grassian, V. H. 2005. Heterogeneous uptake and reactivity of formic acid and calcium carbonate particles: a Knudsen cell reactor, FTIR and SEM study. *Phys. Chem. Chem. Phys.* **7**, 3587–3595.

Andreae, M. O., Charlson, R. J., Bruynseels, F., Storms, H., Van Grieken, R. and co-authors. 1986. Internal mixture of sea salt, silicates, and excess sulfate in marine aerosols. *Science* **232**, 1620–1623.

Arimoto, R., Hogan, A., Grube, P., Davis, D., Webb, J. and co-authors. 2004. Major ions and radionuclides in aerosol particles from the South Pole during ISCAT-2000. *Atmos. Environ.* **38**, 5473–5484.

Atkinson, A. and Whitehouse, M. J. 2001. Ammonium regeneration by Antarctic mesozooplankton: an algometric approach. *Marine Biol.* **139**, 301–311.

Basile, I., Grousset, F. E., Revel, M., Petit, J.-R., Biscay, P. E. and co-authors. 1997. Patagonian origin of glacial dust deposited in East Antarctica (Vostok and Dome C) during glacial stages 2, 4 and 6. *Earth Planet. Sci. Lett.* **146**, 573–589.

Bonsang, B., Martin, D., Lambert, G., Kanakidou, M., Le Roulley, J.-C. and co-authors. 1991. Vertical distribution of nonmethane hydrocarbons in the remote marine boundary layer. *J. Geophys. Res.* **96**, 7313–7324.

Bonsang, B., Polle, C. and Lambert, G. 1992. Evidence for marine production of isoprene. *Geophys. Res. Lett.* **19**, 1129–1132.

Briat, M., Boutron, C. and Lorius, C. 1974. Chlorine and sodium content of East Antarctica firn samples. *J. Atmos. Res.* **8**, 895–901.

Chebbi, A. and Carlier, P. 1996. Carboxylic acids in the troposphere, occurrence, sources, and sinks: a review. *Atmos. Environ.* **30**(24), 4233–4249.

Cosme, E., Hourdin, F., Genthon, C. and Martinerie, P. 2005. The origin of dimethylsulfide (DMS), non-sea-salt sulfate, and methanesulfonic acid (MSA) in Eastern Antarctica. *J. Geophys. Res.* **110**(D3), D03302/1–D03302/17.

Currie, L. A., Kessler, J. D., Fletcher, R. A. and Dibb, J. E. 2005. Long range transport of biomass aerosol to Greenland: multi-spectroscopic investigation of particles deposited in the snow. *J. Radioanal. Nucl. Chem.* **263**(2), 399–411.

De Angelis, M., Barkov, N. I. and Petrov, V. N. 1992. Sources of continental dust over Antarctica during the last glacial cycle. *J. Atmos. Chem.* **14**, 233–244.

De Angelis, M. and Legrand, M. 1995. Preliminary investigations of post depositional effects on HCl, HNO_3, and organic acids in polar firn layers. In: *Ice Core Studies of Global Biogeochemical Cycles* (R. J. Delmas (ed.)) Vol. 30, NATO ASI Series I, Springer-Verlag, Berlin, Heidelberg, pp. 336–381.

De Angelis, M., Simoes, J. C., Bonnaveira, H., Taupin, J. D. and Delmas, R. J. 2003. Volcanic eruptions recorded in the Illimani ice core (Bolivia): 1918-98 and Tambora periods. *Atmos. Chem. Phys.* **3**, 1725–1741.

De Angelis, M., Steffensen, J. P., Legrand, M., Clausen, H. B. and Hammer, C. U. 1997. Primary aerosol (sea salt and soil dust) deposited in Greenland ice during the last climatic cycle: comparison with east Antarctic records. *J. Geophys. Res.* **102**(C12), 26681–26698.

Delmonte, B., Basile-Doelsch, I., Petit, J.-R., Michard, A., Revel-Rolland, M., Maggi, V. and Gemmiti, B. 2003. Refining the isotopic (Sr-Nd) signature of potential source areas for glacial dust in East Antarctica. *J. Phys. IV France* **107**, 365–368.

Dentener, F. J., Carmichael, G. R., Ahang, Y., Lelieved, J. and Crutzen, P. J. 1996. Role of mineral aerosol as a reactive surface in the global troposphere. *J. Geophys. Res.* **101**(D17), 22869–22889.

Dibb, J. E. and Arsenault, M. 2002. Shouldn't snowpacks be sources of monocarboxylic acids? *Atmos. Environ.* **36**, 2513–2522.

Dibb, J. E., Talbot, R. W. and Bergin, M. H. 1994. Soluble acidic species in air and snow at Summit, Greenland. *Geophys. Res. Lett.* **21**, 1627–1630.

Eisele, F., Davis, D. D., Helmigc, D., Oltmans, S. J., Neff, W. and co-authors. 2008. Antarctic Tropospheric Chemistry Investigation (ANTCI) 2003 overview. *Atmos. Environ.* **42**, 2749–2761.

EPICA Community Members. 2006. One to one coupling of glacial climate variability in Greenland and Antarctica. *Nature* **444**, 195–198.

Erbland, J., Savarino, J., Morin, S. and Frey, M. 2009a. Post-depositional processing of nitrate recorded in the Vostok ice core does not care about ice ages. *Geophys. Res. Abs.* **11**, EGU2009-971-1.

Erbland, J., Savarino, J., Morin, S. and Frey, M. 2009b. The oxygen isotope anomaly ($\Delta^{17}O$) of nitrate in the Vostok ice core: insights in the possible changes in NOx oxidation pathways over the last 150 000 years. *Geophys. Res. Abs.* **11**, EGU2009-975.

Fisher, H., Fundel, F., Ruth, U., Twarloh, B., Wegner, A., Udisti, R., and co-authors. 2007. Reconstruction of millennial changes in dust emission, transport and regional sea ice coverage using the deep EPICA ice cores from the Atlantic and Indian Ocean sector of Antarctica. *Earth Planet. Sci. Lett.* **260**, 340–354.

Gao, Y., Anderson, J. R. and Hua, X. 2007. Dust characteristics over the North Pacific observed through shipboard measurements during the ACE-Asia experiment. *Atmos. Environ.* **41**(36), 7907–7922.

Gaudichet, A., de Angelis, M., Joussaume, S., Petit, J.-R., Korotkevich, Y. S. and co-authors. 1992. Comments on the origin of dust in east Antarctica for present and ice age conditions. *J. Atmos. Chem.* **14**, 129–142.

Grosjean, D. 1992. Formic and acetic acids: emissions, atmospheric formation and dry deposition at two Southern California locations. *Atmos. Environ.* **26A**, 3269–3286.

Hatch, C. D., Gough, R. V. and Tolbert, M. A. 2007. Heterogeneous uptake of the C_1 to C_4 organic acids on a swelling clay mineral. *Atmos. Chem. Phys.* **7**, 4445–4458.

Herman, J. R., Krotkov, N., Celarier, E., Larko, D. and Labow, G. 1999. Distribution of UV radiation at the Earth's surface

from TOMS-measured UV backscattered radiance. *J. Geophys. Res.* **104**, 12059–12076.

Jacob, D. 1986. Chemistry of OH in remote cloud sand its role in the production of formic acid and peroxymonosulphate. *J. Geophys. Res.* **91**, 9807–9826.

Jacob, D. J. and Wofsy, S. C. 1988. Photochemistry of biogenic emission over the Amazon forest. *J. Geophys. Res.* **93**, 1477–1486.

Kahl, J. D. W., Martinez, D. A., Kuhns, H., Davidson, C. I., Jaffrezo, J.-L. and co-authors. 1997. Air mass trajectories to Summit, Greenland: a 44-year climatology and some episodic events. *J. Geophys. Res.* **102**(C12), 26861–26875.

Kaufmann, P., Fundel, F., Fischer, H., Bigler, M., Ruth, U. and co-authors. 2010. Ammonium and non-sea salt sulfate in the EPICA ice cores as indicator of biological activity in the Southern Ocean. *Quatern. Sc. Rev.* **29**(1/2), 313–323.

Keene, W. C. and Galloway, J. N. 1984. Organic acidity of precipitation of North America. *Atmos. Environ.* **18**, 2491–2497.

Keene, W. C. and Galloway, J. N. 1988. The biogeochemical cycling of formic and acetic acids through the troposphere: an overview of current understanding. *Tellus* **40**, 322–334.

Keene, W. C., Lobert, J. M., Crutzen, P. J., Maben, J. R., Scharffe, D. H. and co-authors. 2006. Emissions of major gaseous and particulate species during experimental burns of southern African biomass. *J. Geophys. Res.* **111**, D04301. DOI: 10.1029/2005JD006319.

Keene, W. C., Pszenny, A., Galloway, J. and Hawley, M. 1986. Sea-salt corrections and interpretation of constituent ratios in marine precipitation. *J. Geophys. Res.* **91**, 6647–6658.

Kesselmeier, J. and Staudt, M. 1999. Biogenic volatile compounds (VOC): an overview on emission, physiology, and ecology. *J. Atmos. Chem.* **33**, 23–88.

Khare, P., Kumar, N. and Kumari, K. W. 1999. Atmospheric formic and acetic acids: an overview. *Rev. Geophys.* **37**, 227–248.

Kim, B.-G. and Park, S.-U. 2001. Transport and evolution of a winter-time yellow sand observed in Korea. *Atmos. Environ.* **35**, 3191–3201.

Koppman, R., Bauer, R., Johnen, F. R., Plass, C. and Rudolph, J. 1992. The distribution of light nonmethane hydrocarbons over the mid-Atlantic: results of the Polarstern cruise ANT VII/1. *J. Atmos. Chem.* **15**, 215–234.

Kumai, M. 1976. Identification of nuclei and concentrations of chemical species in snow crystals sampled at the South Pole. *J. Atmos. Sci.* **33**, 833–841.

Lefer, B. L., Talbot, R. W., Harris, R. C., Bradshaw, J. D., Sandholm, S. T. and co-authors. 1994. Enhancement of acidic gases in biomass burning impacted air masses over Canada. *J. Geophys. Res.* **99**, 1721–1737.

Legrand, M. 1985. Chimie des neiges et glaces antarctiques: un reflet de l'environnement. PhD Thesis, Université Scientifique et Médicale de Grenoble, France.

Legrand, M. 1995. Sulphur derived species in polar ice: a review. In: *Ice Core Studies of Global Biogeochemical cycles* (R. Delmas (ed.)) Vol. 30, NATO ASI Ser., Ser. I, pp. 91–119. New York: Springer-Verlag.

Legrand, M. and de Angelis, M. 1995. Origins and variations of light carboxylic acids in polar precipitation. *J. Geophys. Res.* **100**(D1), 1445–1452.

Legrand, M. and de Angelis, M. 1996. Light carboxylic acids in Greenland ice: a record of past forest fires and vegetation emissions from the boreal zone. *J. Geophys. Res.* **101**(D2), 4129–4145.

Legrand, M.-R., Lorius, C., Barkov, N. Y. and Petrov, V. N. 1988. Vostok (Antarctica) ice core: atmospheric chemistry changes over the last climatic cycle (160,000 yrs). *Atmos. Environ.* **22**(2), 317–331.

Legrand, M. and Mayewsky, P. 1997. Glaciochemistry of polar ice cores: a review. *Rev. Geophys.* **35**(3), 219–243.

Legrand, M. and Wagenbach, D. 1999. Impact of the Cerro Hudson and Pinatubo volcanic eruptions on the Antarctic air ad snow chemistry. *J. Geophys. Res.* **104**(D1), 1581–1596.

Legrand, M., Wolff, E. and Wagenbach, D. 1999. Antarctic aerosol and snowfall chemistry: implications for deep Antarctic ice-core chemistry. *Ann. Glaciol.* **29**, 66–72.

Legrand, M., Preunkert, S., Jourdain, B. and Aumont, B. 2004. Year-round records of gas and particulate formic and acetic acids in the boundary layer at Dumont D'Urville, coastal Antarctica. *J. Geophys. Res.* **109**(D06313), 1–11.

Legrand M., Preunkert, S., Wagenbach, D., Cachier, H. and Puxbaum, H. 2003. A historical record of formate and acetate from a high-elevation Alpine glacier: implications for their natural versus anthropogenic budgets at the European scale. *J. Geophys. Res.* **108**, 244788. DOI: 10.1029/2003JD003594.

Littot, G. C., Mulvaney, R., Röthlisberger, R., Udisti, R., Wolff, E. W. and co-authors. 2002. Comparison of analytical methods used for measuring major ions in the EPICA Dome C (Antarctica) ice core. *Ann. Glaciol.* **35**, 299–305.

Loulergue, L., Schilt, A., Spahni, R., Masson-Delmotte, V., Blunier, T., Lemieux, B. and co-authors. 2008. Orbital and millennial-scale features of atmospheric CH4 over the last 800,000 years. *Nature* **453**, 383–386.

Madronich, S. and Calvert, J. G. 1990. Permutation reaction of organic peroxy radicals in the troposphere. *J. Geophys. Res.* **95**, 5697–5715.

Madronich, S., Chatfield, R. B., Calvert, J. G., Moortgat, G. K., Veyret, B. and co-authors. 1990. A photochemical origin of acetic acid in the troposphere. *Geophys. Res. Lett.* **17**(12), 2361–2364.

Matsumoto, K., Nagao, I., Tanaka, H., Miyaji, H., Iida, T. and co-authors. 1998. Seasonal characteristics of organic and inorganic species and their size distributions in atmospheric aerosols over the northwest Pacific Ocean. *Atmos. Environ.* **32**(11), 1931–1946.

Moreno Rivadeneira, I. 2011. *Natural Variability of the Atmospheric Composition and Anthropogenic Influence in Patagonia. Contribution to the Understanding of Transport Pathways Along the Equator-Mid Latitudes-Pole Transect*. PHD Thesis, Université de Grenoble, France.

Ooki, A. and Uematsu, M. 2005. Chemical interactions between mineral dust particles and acid gas during Asian dust events. *J. Geophys. Res.* **110**, D03201. DOI: 10.1029/2004JD004737.

Paulot, F., Wunch, D., Crounse, J. D., Toon, G. C., Millet, D. B. and co-authors. 2011. Importance of secondary sources in the atmospheric budgets of formic and acetic acids. *Atmos. Chem. Phys.* **11**, 1989–2013.

Piel, C., Weller, R., Huke, M. and Wagenbach, D. 2006. Atmospheric methane sulfonate and non-sea-salt sulfate records at the European Project for Ice Coring in Antarctica (EPICA) deep-drilling site in Dronning Maud Land, Antarctica. *J. Geophys. Res.* **111**, D03304. DOI: 10.1029/2005JD006213.

Preiss, N., Melières, M.-A. and Pourchet, M. 1996. A compilation of data on lead 210 concentrations in surface air and fluxes at the air-surface and water-sediment interfaces. *J. Geophys. Res.* **101**(D22), 28847–28862.

Pretzler Prince, A., Kleiber, P. D., Grrassian, V. H. and Young, M. A. 2008. Reactive uptake of acetic acid on calcite and nitric acid reacted calcite aerosol in an environmental reaction chamber. *Phys. Chem. Chem. Phys.* **10**, 142–152.

Preunkert, S., Jourdain, B., Legrand, M., Udisti, R., Becagli S. and co-authors. 2008. Seasonality of sulfur species (dimethyl sulfide, sulfate, and methanesulfonate) in Antarctica: inland versus coastal regions. *J. Geophys. Res.* **113**, D15302. DOI: 10.1029/2008JD009937.

Röthlisberger, R., Hutterli, M. A., Sommer, S., Wolff, E. W. and Mulvaney, R. 2000. Factors controlling nitrate in ice cores: evidence from the Dome C deep ice core. *J. Geophys. Res.* **105**, 20565–20572.

Ruth, U., Barnola, J.-M., Beer, J., Bigler, M., Blunier, T. and co-authors. 2007. EDML1: a chronology for the EPICA deep ice core from Dronning Maud Land, Antarctica, over the last 150 000 years. *Clim. Past*, **3**, 475–484.

Savarino, J. and Legrand, M. 1998. High northern latitude forest fires and vegetation emissions over the last millennium inferred from the chemistry of a Central Greenland ice core. *J. Geophys. Res.* **103**(D7), 8267–8279.

Singh, H. B., Viezee, W., Chen, Y., Bradshaw, J., Sandholm, S. and co-authors. 2000. Biomass burning influences on the composition of the remote South Pacific troposphere: analysis based on observations from PEM6Tropics-A. *Atmos. Environ.* **34**, 635–644.

Staffelbach, T., Neftel, A., Stauffer, B. and Jacob, D. 1991. A record of the atmospheric methane sink from formaldehyde in polar ice cores. *Nature* **349**, 603–605.

Talbot, R. W., Beecher, K. M., Harris, R. C. and Cofer, W. R. 1988. Atmospheric geochemistry of formic and acetic acids at a mid-latitude site. *J. Geophys. Res.* **93**, 1638–1652.

Talbot, R. W., Andreae, M. O., Berresheim, H., Jacob, D. J. and Beecher, K. M. 1990. Sources and sinks of formic, acetic, and pyruvic acids over Central Amazonia: 2. Wet season. *J. Geophys. Res.* **95**, 16799–16811.

Tissari, J., Sippula, O., Vuorio, K. and Fokiniemi, J. 2008. Fine particle and gas emissions from the combustion of agricultural fuels fired in 20 kW burner. *Energy Fuels* **22**, 2033–2042.

Traversi, R., Becagli, S., Castellano, E., Cerri, O., Morganti, A. and co-authors. 2009. Study of the Dome C site (East Antarctica) variability by comparing chemical stratigraphies. *Microchem. J.* **92**(1), 7–14.

Tuncel, G., Aras, N. K. and Zoller, W. H. 1989. Temporal variations and sources of elements in the south pole atmosphere 1. Nonenriched and moderately enriched elements. *J. Geophys. Res.* **94**(D10), 13025–13038.

Vimeux, F., De Angelis, M., Ginot, P., Magand, O., Casassa, G. and co-authors. 2008. A promising location in Patagonia for paleoclimate and paleoenvironmental reconstructions revealed by a shallow firn core from Monte San Vanlentin (Northern Patagonia Icefield, Chile). *J. Geophys. Res.* **113**, D16118. DOI: 10.1029/2007JD009502.

Voisin, D., Legrand, M. and Chaumerliac, N. 2000. Scavenging of acidic gases (HCOOH, CH3COOH, HNO3, HCl, and SO2) and ammonia in mixed liquid-solid water clouds at the Puy de Dome Mountain (France). *J. Geophys. Res.* **105**(D5), 6817–6835.

Weller, R., Traufetter, F., Fisher, H., Oerter, H., Piel, C. and co-authors. 2004. Post depositional losses of methane sulfonate, nitrate, and chloride at the European Project of Ice Coring in Antarctica deep-drilling site in Dronning Maud Land, Antarctica. *J. Geophys. Res.* **109**, D07301. DOI: 10.1029/2003JD004189.

Winchester, J. W. and Wang, M.-X. 1989. Acid-base balance in aerosol components of the Asia-Pacific region. *Tellus.* **41B**(3), 323–337.

Wolff, E. W., Fisher, H., Ruth, U., Twarloh, B., Littot, G. C., Mulvaney, R. and co-authors. 2006. Southern Ocean sea-ice extent, productivity and iron flux over the past eight glacial cycles. *Nature* **440**, 491–496.